2015

# Design of an All-In-One Embedded Flight Control System

Joel D. Elmore
*Virginia Commonwealth University*

# Design of an All-in-One Embedded Flight Control System

A thesis submitted in partial fulfillment of the requirements for the degree of Master of Science at Virginia Commonwealth University.

by

Joel D. Elmore

Director: Dr. Robert H. Klenke
Professor of Electrical & Computer Engineering

Virginia Commonwealth University
Richmond, Virginia
August 2015

# Acknowledgments

Many people helped in their guidance and support to make this work possible. I would first like to acknowledge my advisor, Dr. Robert H. Klenke, for his oversight and support. His enthusiasm and desire to explore the technologies within the field of unmanned aerial systems helped motivate this project to its fruition. I would also like to thank my committee members, Dr. Jayasimha Atulasimha and Dr. Alen Docef, for their advice and feedback on my work. I would like to express my sincerest appreciation towards my family for their encouragement and support during my studies. Finally, I would like to thank my closest friends, Garrett and Viktor, for their friendship and keeping most of my ideas grounded in reality, which is the real reason this thing doesn't brew in-flight coffee.

# Contents

# List of Figures

# List of Tables

# List of Abbreviations

| | |
|---|---|
| BEC | Battery Equivalent Circuit |
| BIST | Built in Self Test |
| DSP | Digital Signal Processors |
| EKF | Extended Kalman Filter |
| EMC | Electromagnetic Compatibility |
| EOL | End-of-Life |
| ESC | Electronic Speed Controller |
| ESL | Effective Series Inductance |
| ESR | Effective Series Resistance |
| FCM | Flight Control Module |
| FFT | Fast Fourier Transform |
| FOV | Field of View |
| FPGA | Field-Programmable Gate Array |
| FPU | Floating Point Unit |
| GCS | Ground Control Station |
| HILS | Hardware in the Loop Simulation |
| HSE | High Speed External |
| IC | Integrated Circuit |
| ICM | Instrumentation Control Module |
| IMU | Inertial Measurement Unit |
| LDO | Low-Dropout |

| | |
|---|---|
| LGA | Lead Grid Array |
| LwIP | Lightweight IP Stack |
| MDI-X | Medium Dependent Interface Crossover |
| MEMS | Micro-Electro-Mechanical System |
| MII | Media-Independent Interface |
| NDA | Non-Disclosure Agreement |
| NMEA | National Marine Electronics Association |
| NSMD | Non Solder Mask Defined |
| NVM | Non-Volatile Memory |
| OTG | On-The-Go |
| PCB | Printed Circuit Board |
| PFM | Pulse Frequency Modulation |
| PGS | portable ground station |
| PHY | Physical Interface Device |
| POT | Patch On Top |
| PWM | Pulse Width Modulation |
| QFN | Quad Flat No-Lead |
| RC | Remote Controlled |
| RMII | Reduced Media-Independent Interface |
| RTC | Real Time Clock |
| RTF | Ready to Fly |
| RTOS | Real-Time Operating System |
| SDHC | Secure Digital High Capacity |
| SDIO | Secure Digital Input/Output |
| SMD | Solder Mask Defined |
| SPI | Serial Peripheral Interface |
| TEB | Total Error Band |

| | |
|---|---|
| TTL | Transistor-Transistor Logic |
| UAS | Unmanned Aerial System |
| UAV | Unmanned Aerial Vehicle |
| USB | Universal Serial Bus |
| VCU | Virginia Commonwealth University |

# Abstract


DESIGN OF AN ALL-IN-ONE EMBEDDED FLIGHT CONTROL SYSTEM

Joel D. Elmore

A thesis submitted in partial fulfillment of the requirements for the degree of Master of Science at Virginia Commonwealth University.

Virginia Commonwealth University, 2014

Director: Dr. Robert H. Klenke, Professor of Electrical & Computer Engineering

This thesis describes an all-in-one flight control system (FCS) that was designed for unmanned aerial vehicles (UAVs). The project focuses on the embedded hardware aspect of a stand-alone system with low-cost and reliability in mind.

# Chapter 1: Introduction

## 1.1 Overview

Over the past years unmanned systems have established a presence in the consumer market, removing the barriers that have bound them strictly to military and research environments. The advances in processing power over dissipated power created the ability to develop low-cost, high performance hardware capable of running intensive algorithms within limited space and power constraints. This created new opportunities that have seen an explosion of interest and development. The potential for unmanned systems has been established and their use will only continue to grow in new and exciting ways.

One of the major advantages of unmanned systems is the removal of a human operator from the vehicle. This creates interesting applications that otherwise would be too dangerous or costly to require human presence on board. The obvious uses like reconnaissance and surveillance are actively being deployed among military and law enforcement. More notable, the onset of civilian interest is beginning to take shape in a diverse field of applications. Amazon's push for same-day delivery using Unmanned Aerial Vehicle (UAV)s explores this option with the attempt to bring the use of UAVs to an everyday occurrence. Driverless car technology being developed by automotive companies such as BMW and Volvo, also promise routine interaction with unmanned systems. The continued development of unmanned systems will enable evermore advanced and integrated platforms, proficient at diverse situations and missions.

## 1.2 Motivation

A few years ago, most autopilot systems were out of reach of the consumer; the cost was simply too high. Today, powerful inexpensive microprocessors with a variety of peripheral capabilities have created the possibility for cheap, feature-rich autopilots. The variety of available autopilot hardware and software solutions continue to grow each bringing forth its own varying capabilities. However, majority of these units do not provide an all-in-one embedded capability for robust flight control. They often require several external sensors, complicating in-field setup and increasing airframe size.

There have been several iterations of autopilot solutions developed at Virginia Commonwealth University (VCU) UAV lab. Two of these systems are still in active use. The two platforms carry their own set of features and drawbacks. One was developed for research in complex flight control algorithms, while the other was designed for simplicity and lower cost. Both autopilot systems will be further discussed in Chapter 2.

Both existing VCU systems are based on older microprocessor technology and both have shortcomings that led to the desire to create an entirely new platform. This new platform is designed to be the best of both worlds, offering a low cost solution that is still powerful enough for research. To decrease reliance on external systems, one of the primary motivators was to integrate all necessary sensors and communications with the overall system.

## 1.3 Problem Statement

Analyzing the requirements for VCU's flight control hardware, the need for two different solutions became apparent. A large, feature-rich system was designed to accommodate all sensors necessary for flight, while providing high connectivity and customization. There was also a need for a smaller, cheaper version of the current system, while still maintaining the same respective feature set and improved performance. With a smaller form factor and less additional add-on requirements, lighter and more compact airframes can be used, which in turn saves cost. This was desirable for the purpose of research into collaborative UAV operations using low-cost vehicles.

The custom Printed Circuit Board (PCB)s enable a precise fitting for our research needs, as current available systems do not meet the necessary capability. The goal was to provide a complete suite of sensor and communication hardware into single board solutions. Both platforms share a common set of core sensors, with the more sophisticated of the two offering more features at the expense of physical size and power requirements.

## 1.4 Organization

This thesis is organized as followed. Chapter 2 provides an overview of existing small UAV hardware in both open source and commercial systems. Chapter 3 describes details of the physical component choices and their respective purpose. Chapter 4 provides a complete overview of the board design as well as a detailed description for the PCB layout and geometries. Chapter 5 illustrates the complete system in use and performance characteristics. Chapter 6 summarizes the performance and characteristics of the system in use and outlines suggestions for future development.

# Chapter 2: Background

This chapter overviews various commercial autopilot systems, including previous generations of VCU autopilots. Each system's characteristics and features will be discussed. System flexibility and supported configurations will also be mentioned.

## 2.1 Hobbyists Autopilot Systems

Within the past few years the Remote Controlled (RC) hobbyists and UAV enthusiast communities have been developing increasingly more powerful autonomous platforms. Unmanned flight is no longer strictly constrained to big budget agencies or universities. Complete Ready to Fly (RTF) UAV aircrafts have even made their way to local hobby shops, such as the DJI Phantom multirotor aircraft [11]. While the Phantom is a closed system and cannot be significantly modified, there are several autopilots amongst the open-source community that offer a wide range of end-user modification options.

### 2.1.1 Paparazzi

The Paparazzi Unmanned Aerial System (UAS) project aims to develop a versatile and user-friendly autopilot with a wide set of supported vehicles [12]. Its development was started at the ENAC University in France. All project hardware and software was released under the GNU GPL (which one?) license agreement, making the system fully customizable for individual needs and purposes

The source code is written in C and abstracted from the hardware for easy configuration amongst platforms. All core system parameters (Airframe, Flight Plan, Radio, Telemetry, and Settings) are conveniently modifiable through XML files. This allows for quick porting to new airframe or flight modes. The system does fall short when further customization goes beyond the predefined XML files, although most configurations and additional hardware support can be implemented with a deep understanding of the software structure. Currently, a large list of sensor hardware is supported, notably several Inertial Measurement Unit (IMU)s.

The array of available system hardware is increasingly diverse, enabling its use among several applications. Newer hardware being delivered is trending towards STMicroelctronic's 32-bit ARM processors. Two of the more updated autopilots are the KroozSD and the Apogee [12]. Each solution holds its own set of strengths and weaknesses, but are both very capable at fulfilling their niched purpose. The two integrated autopilots utilize the same STM32F405RG6 processor running at 168MHz.

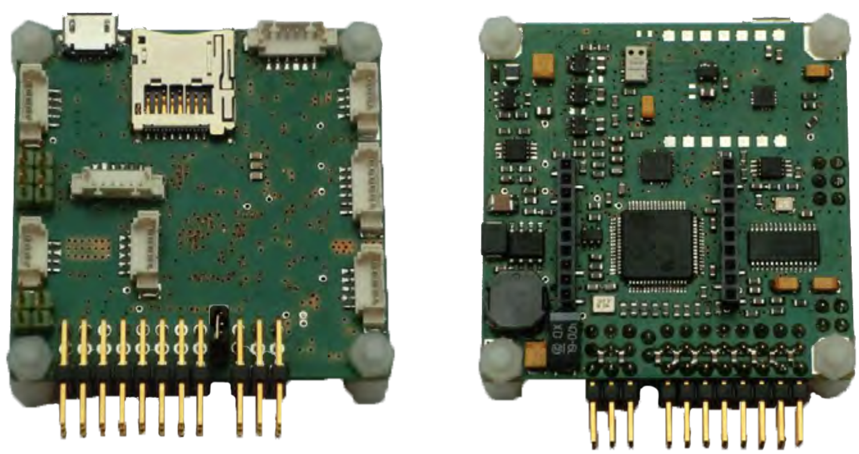

Figure 2.1: KroozSD Autopilot, top view on left and bottom view on right. [1]

The KroozSD shown in Figure 2.1 measures a square 1.97" by 1.97" excluding the right angle PWM headers [1]. Its intended purpose is geared towards multirotor use, although it can be outfitted for fixed wing flight. The board utilizes the 64-pin STM32F405RGT6 processor clocked at 168MHz. It carries with it a suite of sensor and communication hardware (9-axis IMU, barometric pressure sensor, and XBee), enabling flight with only an external GPS module. The IMU comprises of three separate Integrated Circuit (IC)s: MPU6050 gyro/accelerometer, MXR9500 accelerometer with a 16-bit ADC, and HMC5883 magnetometer. The barometric sensor (MS5611) is a non-ported, high resolution sensor with 10cm accuracy [13]. Flight data logging to an SD card is available, although not all SD cards support the implemented Serial Peripheral Interface (SPI) circuitry.

The KroozSD can utilize up to eleven Pulse Width Modulation (PWM) outputs with Futaba's S-BUS protocol. It does boast a large input supply voltage (up to $35V$), capable of supporting an eight cell LiPo.

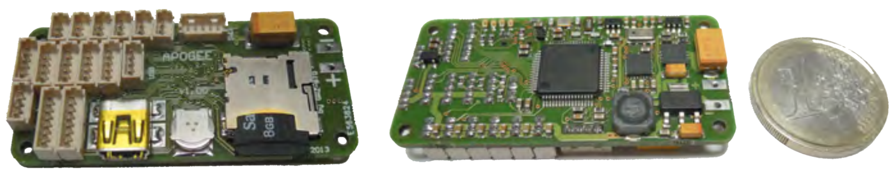

Figure 2.2: Apogee Autopilot V1.00, top view on left and bottom view on right. [2]

Similar to the KroozSD, the Apogee includes on-board sensors for flight (IMU and barometric pressure sensor), while featuring a more compact design, measuring 2.1" by 0.98" [2]. The smaller size came at the cost of several output channels and the XBee. However, there are several a few improvements over the KroozSD, such as faster data logging to the SDcard (through SDIO) and an Real Time Clock (RTC) with backup capacitor.

The notable shortcomings amongst these systems are the lack of dedicated safety-switch circuitry. They rely heavily on the stability of the flight control software, using prioritized threads. In the event of failure, full control of the aircraft is lost. The on-board barometric pressure sensor is non-ported causing issues in enclosed spaces where static pressure inside the aircraft builds during flight.

### 2.1.2 Pixhawk

The Pixhawk Autopilot (shown in Figure 2.3) project by 3DRobotics took a similar approach to the Paparazzi; both software and hardware are made open-source (under the BSD licensing)

Figure 2.3: 3DR Pixhawk Autopilot [3]

target a similar community. The project offers a complete solution for the embedded software and Ground Control Station (GCS) while also supporting the Ardupilot software suite (a popular autopilot among hobbyist). [3]

The autopilot hardware includes a similar processor (STM32F4) to the KroozSD and Apogee boards, but with the added benefit of a hardware accelerated cryptography core. While not implemented, this feature adds the potential capability of a secure ground link. A built-in IMU and non-ported altimeter is incorporated into the autopilot, but all other sensory and communication necessary for flight are externally connected. An external compass is made available if electromagnetic noise affects the on-board magnetometer due to motors and power wiring. Unlike the Paparazzi, a dedicated safety processor ensures manual override of the autopilot in the event the flight controller's processor fails or locks up. A complete setup costs a little under $450, making it one of the more expensive autopilots in this category.

The Pixhawk offers some unique capabilities that set it apart from other solutions in its category. 3DRobotics developed (PX4FLOW) an optical flow camera coupled with an ultra sonic distance sensor to achieve accurate position estimation in situations with inadequate or unavailable GPS data [14]. Micro aerial vehicles have successfully used optical computer mice to achieve similar navigation capabilities, however this approach often requires several sensors to broaden the range. PX4FLOW offers a single low-cost, low-power CMOS sensor with a 21 degree Field of View (FOV) and 752x480 resolution. The range sensor is used for scene distance calculation for scaling optical flow measurements to metric velocity. Induced error from angular velocity is mitigated through gyroscope compensation. An on-board STM32F4 processes the sensor data and makes it available via I2C. The end result yields high dead-reckoning accuracy unavailable to similar autopilots.

## 2.2 Commercial Off the Shelf Autopilots

In this section, a few common autopilots will be compared in terms of microcontroller, sensors, and overall cost. Due to the closed, propriety nature of commercial autopilots, specific details allowing a full comparison were difficult to obtain.

### 2.2.1 Cloud Cap Technology

Figure 2.4: Piccolo Autopilots: Piccolo Nano (Right), Piccolo SL (Middle), and Piccolo II (Left) [4]

Cloud Cap Technology currently provides three commercially available autopilots under the Piccolo brand name (Piccolo II, Piccolo SL, and Piccolo Nano), displayed in Figure 2.4 [4]. The Piccolo autopilots include a complete off the shelf solution comprising the core flight controller, navigation, sensors, wireless communication and payload interfaces. Each Piccolo package shares a common firmware and supporting software, allowing easier maintenance amongst versions. The shared portable ground station (PGS) supports multi-management of autopilots as well as Hardware in the Loop Simulation (HILS) [15].

The Piccolo II provides extensive connectivity and peripheral interfacing options [16]. Excluding the connectors, the unit measures 5.16” by 2.46” by 1.81” and weighs 220 grams. The power supply can handle 8 to 20 volts with a typical power draw of 4 watts. It offers 16 configurable

GPIO lines, of which four can be setup as 10-bit analog inputs, and 5 RS232 payload interfacing options. Its sensor suite includes a 3-axis gyroscope (300 deg/sec), 3-axis accelerometer (10g), uBlox GPS (4 Hz), and ported static and differential pressure sensors (155 kts max). External support for a magnetometer and a laser altimeter is made available for more accurate AHRS. The integrated RF module can be selected in a number of radio frequencies including unlicensed bands 900MHz and 2.4GHz

The Piccolo SL exhibits an aggressively compact form factor while maintaining the same performance as the Piccolo II[17]. It targets small hand-launched airframes or VTOL platforms, where weight reduction is crucial. The unit measures 4.64" by 2.19" by 0.75", and weighs 110 grams. The power supply input voltage range saw a significant improvement (4.5 to 28 volts), however the power draw still remains at 4 watts. The integrated radio sustains the same modem options despite its size. In comparison, the only drawback to the Piccolo SL over the Piccolo II is the fewer payload interface options, such as fewer GPIO (14) and RS232 (3).

The Piccolo Nano is the latest installment to the Piccolo autopilot family [18]. To reduce weight and achieve a small footprint, it forgoes an enclosure and sacrifices GPIO and other connectivity options. The complete autopilot comprises of 3 separate boards (Avionics, GPS, and Radio). The avionics board alone measures 1.8" by 3.0" and weighs 22 grams. However, the collective weight of the system weighs 64 grams. The entire system power draw is not made available, but its input voltage is expanded compared to previous Piccolo autopilots (6 to 30 volts).

### 2.2.2 Lockheed Martin Procerus Technologies

The Kestrel autopilot was developed by Lockheed Martin Procerus Technologies for both fixed wing and VTOL aircrafts [5]. Figure 2.6 demonstrates the small form factor weighing 24 grams and measuring 2.26" by 1.46" by 0.67". The module includes a full inertial sensor set with temperature compensated 3-axis gyroscope, 3-axis accelerometer, 3-axis magnetometer, high precision static pressure, and dynamic pressure sensors. Other accommodating on-board hardware are a GPS and a Microhard Nano modem. The Kestrel V3.1 has a 500MHz DSP with 32Mb flash and 32Mb

Figure 2.5: Kestrel Autopilot V3.1 [5]

RAM as well as an SD card for extended data logging. Among the available IO options are 51 pin wiring harness, 13 servo control pins, 10 ADC inputs, 4 UARTs (GPS, modem, (2) payload), 5 capture compare timer channels, and a 2 Amp GPIO. Further GPIO and serial expansion can be made through a connecting daughter board.

The DSP performs all the control algorithms as well as a 17 state Extended Kalman Filter (EKF) for the INS solution [19]. Built-in autonomous take-off and landing, aggressive ascent and descent, altitude and airspeed hold, and dynamic waypoint navigation capabilities are fully adopted into the FCS. The Kestrel control algorithms rely on traditional PID controllers, which are fully configurable during flight. Procerus also makes real-time performance graphs available within their GCS to aid in-flight parameter tuning.

### 2.2.3 MicroPilot

Figure 2.6: MicroPilot MP2x28 Autopilot [6]

MicroPilot has designed a single flight control board that varies functionality through software licensing [6]. Four basic models exist within the MP2x28g2 family. The autopilots performance vary significantly depending on the licensing. The flight control board weighs 28 grams and measures 3.94” x 1.57” x 0.59”. Its input voltage range tolerates 6.5$V$ to 30$V$ and draws 192$mA$ at 6.5$V$. All models support fixed wing and multi-rotor control, but only the most expensive model includes support for a helicopter. It is this version (MP2128g2Heli) that offers any distinguishable performance competition among other commercially available flight control systems.

The MP2128gHeli’s notable attributes include: tumble recovery and autorotation control dynamics, visioning system, and complete sensor IMU solution (3-axis gyroscope, 3-axis accelerometer, and 3-axis magnetometer). None of these features are available on their lower-end models [20]. The next model down (MP2128g2) does share some high-end features such as, offering the same number of GPIO and servo options (24 with configurable update rates between 50 and 400$Hz$). Dead reckoning navigation through GPS outages is also available. MicroPilot’s basic model excludes most expansion and customization options as well as the ability to add and remove waypoints during flight.

## 2.3 VCU Autopilot Systems

Since its inception, the VCU UAV lab has designed custom hardware and software UAS solutions. We focus on the marriage these two technologies have at the heart of UAS development. Balancing both allows the lab to nimbly respond to the ever-changing research field. The approach produces effective, custom fit designs centered around the problem.

There have been a number of FCS hardware platforms developed at VCU since the beginning of the UAV lab. For the most part, these were always based on Field-Programmable Gate Array (FPGA)s, sometimes paired with a non-FPGA microcontroller. This includes the Suzaku FCS [21], which used a Vertex-II FPGA from Xilinx and ran a form of embedded Linux, and the NextGen FCS [22], one of the systems that was in use prior to the new autopilot described herein, which ran two FPGAs in parallel. In addition, a smaller system, the miniFCS, was also in use prior to the new autopilot. This system only had a microcontroller, and was smaller and cheaper.

## 2.3.1 NextGen FCS

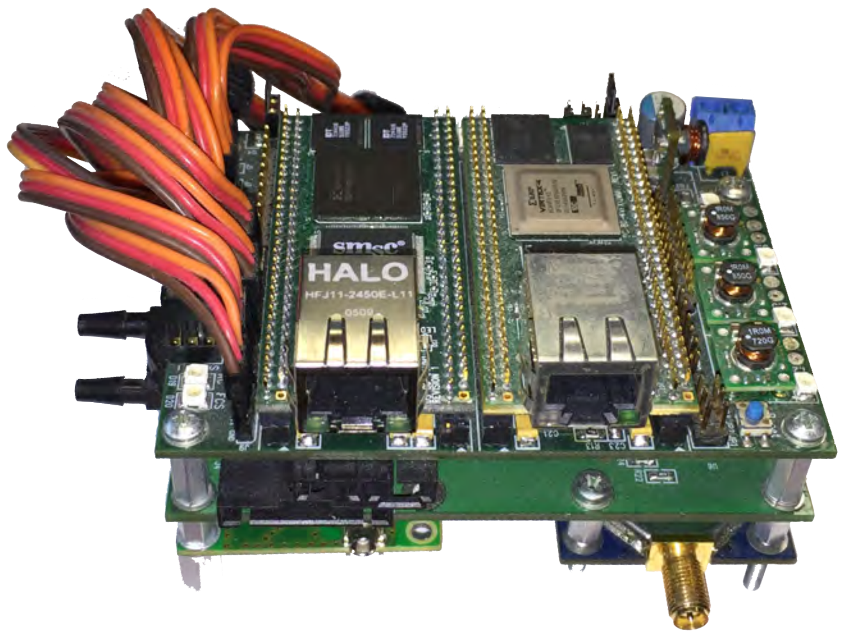


Figure 2.7: Fully assembled NextGen FCS with all peripheral modules.

The NextGen FCS was designed with performance and expandability in mind [22]. It features an impressive array of hardware, including two FPGAs, and features numerous on-board peripherals. Overall cost was not a large consideration for the design of the NextGen; it was primarily designed to be as powerful as possible while still fitting in a small plane.

The hardware for the NextGen is designed around a board stack, using two Xilinx mini-modules for the two FPGAs, a main board, an aux board, and several daughter cards for the aux board. All told, a "fully equipped" NextGen system consists of at least six individual PCBs of varying complexity with dimensions measuring 3.8 by 3.0 by 2.75.

The backbone for the NextGen are the two PCBs which were designed in-house as part of the work in [22]. A two board solution was chosen to preserve space constraints while allowing for future expansion at a relatively low cost. The main board contains the core components of the flight control system: those which are both expensive (the FPGAs, power regulating circuits, etc) and necessary (safety switch, servo controls) for the FCS to function. The aux board contains all the on-board sensors for the FCS: analog barometric sensors and GPS and Modem connections. Although this never transpired, the goal of the aux board was that it would be easily replaced when newer sensor technology was needed/desired, or even be swapped out among a range of different aux boards for different tasks.

The main board is a relatively complicated PCB. It is a six-layer board, with dedicated $3.3V$ and ground planes, two internal planes used for $2.5V$ and $1.8V$ power as well as high-speed signals, and two external planes used for low-speed signals and components. The on-board power system accepts anywhere from 7 to $14V$ inputs, and using a two-stage design converts input voltage to $5.5V$ and from there to the $3.3V$, $2.5V$, and $1.8V$ needed for the on-board components. The main board also contains all servo inputs and outputs, the safety switch, and a bank of status LEDs, as well as GPIO and RS-232 connections for external peripherals.

In contrast, the aux board is somewhat simpler. It is only a four-layer board, with the two internal layers being dedicated power and ground planes. The aux board contains both analog and RF components, and care was taken to isolate these systems as much as possible. There are no on-board RF components as such: the GPS and modem are attached as separate daughterboards to the bottom of the aux board. The aux board also includes a dedicated, low-noise analog power supply, analog pressure sensors, and external inputs for additional analog sensors.

As mentioned, the main board contains both FPGAs. These are on daughterboards of their own, called mini-modules. Each mini-module contains an FPGA and the supporting components (RAM, flash, oscillators), as well as an on-board Ethernet jack with the necessary hardware components. There are two separate FPGAs available, each fulfilling a different need: a Xilinx Spartan-3 FPGA and a Xilinx Virtex-4 FPGA. The former, known as the Instrumentation Control Module (ICM) handles all sensor and ground IO tasks, while the latter, known as the Flight Control Module (FCM) handles the guidance and control algorithms for the FCS.

This division of labor allows the FCM to focus solely on running complex flight control algorithms while the ICM handles resource-intensive IO tasks. The Virtex-4 FPGA on the FCM contains, in addition to the FPGA components, a PowerPC 405 CPU core. Combined with the

64MB of on-module RAM, the Virtex-4 is powerful enough to run an embedded version of Linux, enabling the design of the flight control software to be simplified to a Linux program. The ICM contains a less-powerful FPGA with no integrated processor; instead, a soft-core Microblaze processor is used. This processor is implemented using the FPGA itself, and does not support an OS.

While the NextGen is a very powerful system, it has several drawbacks which limited its usefulness. It is very large and can draw up to an amp of current at $12V$ when all optional accessories are in use. In addition, while the ICM is relatively easy to update, the FCM suffers from maintainability problems due to the way Linux was implemented for the platform. This greatly reduced the ability of the UAV lab to take advantage of the processing power available in the system. While the NextGen was very adept at flying larger planes, it was not suitable for long-term research.

### 2.3.2 MiniFCS


Figure 2.8: Top View of miniFCS Autopilot [7]

Due in large part to the high cost of the NextGen, as well as wanting a smaller platform for smaller foam gliders, a second, low-cost system was developed alongside the NextGen [8]. The miniFCS shown in Figure 2.8 was designed from the beginning to be inexpensive and small: cost targets for the initial version were $250, with a power budget of 100mW and a size of around a credit card. This system was designed to go into a small airframe, so components and sensors were chosen to allow for as small a system as possible while keeping everything on one board.

The miniFCS is a single processor system, based on the Atmel AVR32 UC3 processor. This processor is much less powerful than the NextGen's processor, but still capable of running the basic sensor and control algorithms used by the UAV lab. It lacks a Floating Point Unit (FPU) and a large variety of IO options, which somewhat limits its usefulness in new development.

As the miniFCS was designed to be size constrained, the six PCBs of the NextGen were reduced to two: the main miniFCS board and an optional on-board Xbee modem for ground communications. The miniFCS also does away with an integrated GPS, instead relying on an external GPS module that can be powered and connected to the miniFCS with a single cable. Like the NextGen, analog pressure sensors are used; the ones chosen for the miniFCS have a much more limited range and resolution than the NextGen, which limits the miniFCS to flying at relatively low altitudes on barometric sensors alone.

Unlike the NextGen, which requires an expensive external IMU, the miniFCS has support for a low-cost, built-in attitude solution in the form of analog IR sensors. These sensors give a rough estimation of attitude based on the background infrared radiation of the sky and ground. Although not particularly accurate, these sensors are usually sufficient for flight.

The miniFCS is much more maintainable than the NextGen; however, it suffers in other ways. The on-board processor is not powerful enough to perform both flight control and sensor fusion algorithms simultaneously, especially as it lacks a floating point unit. It lacks in IO expansion as well, requiring a mess of jumper wires to expose additional sensor interfaces when needed. Additionally, the miniFCS does not use the same flight control algorithms as the NextGen, and tends to perform worse in larger planes than the NextGen does.

## 2.4 Software Overview

The software for the new autopilot (named Aries) was developed as part of the previous work shown in [23]. However, since that work was written, the software for Aries was completely re-written to take advantage of a Real-Time Operating System (RTOS) which enables additional functionality of the Aries board. A brief overview of the current software is given below.

The Aries/RT software is a fundamentally different platform than the Aries software developed in [23] and used for the first two revisions of the Aries board. Aries/RT is based on the freely-available RTOS ChibiOS/RT [24], a lightweight RTOS targeted specifically at low-cost ARM processors that have become ubiquitous in the past 5 years. The use of an RTOS brings several major improvements over the previous Aries software platform: proper scheduling and context switches; built-in support for Lightweight IP Stack (LwIP) and FatFs, enabling the use of onboard Ethernet and Micro SD cards, respectively; and the removal of several thousand lines of custom hardware drivers at the processor level.

ChibiOS/RT uses a thread-based model to handle tasks. As such, most tasks which were executed by the rudimentary scheduler in the old Aries code are now replaced with threads. Threads are spawned during platform initialization and awoken as needed, either from external events (interrupts, other threads, etc), or on a periodic basis using timers. The addition of threads was a primary motivation for switching to ChibiOS/RT. Without the ability to context switch during an IO-bound operation (for example, an SD card write), performance of the old software was unacceptably low when advanced IO peripherals were added.

As mentioned, the use of an RTOS allows Aries/RT to support new peripherals which, while present on early versions of the Aries hardware, were unable to be used effectively. Two of the major new features enabled by Aries/RT are Ethernet and Micro SD card support. The latest revision of the Aries has the necessary connections to support USB device mode as well, support for this does not currently exist in Aries/RT.

Ethernet support is provided by both ChibiOS/RT (at the MAC level) and LwIP (at the protocol and higher level). This enables the board to have full IPv4 connectivity. While many applications are possible, currently this is used for two things: telemetry and a simple status webpage. Its use for telemetry is the more interesting of the two. This allows for multiple Aries boards to communicate with a GCS on the same network, without needing physical serial modems for all devices. This allows for much easier multi-FCS HILS simulation, and also simplifies programming by eliminating the need for serial modems or FTDI chips.

MicroSD card support is again provided by two libraries: ChibiOS/RT driving the SDC hardware on the STM32, and the FatFS library controlling higher level access to the filesystem on the SD card. Additionally, a third-party wrapper around FatFS, written specifically for ChibiOS/RT, leverages ChibiOS/RT's message queues to allow for safe multi-threaded access to the filesystem; given the relatively slow IO speeds for the SDC, this is necessary to allow for multiple file IO.

A new logging system was written to take advantage of the newly available SD card. By default, a log of all messages printed to the debugging console is saved to the SD card. Despite now having a battery-backed RTC, there are no guarantees that the time is accurate, so the files are created in numbered folders instead of using the current date/time. Additional log files can be opened and stored in the same folder, and the log system supports both raw binary and record (ordered, timestamped binary data) formats in addition to ASCII text. To ensure data integrity in the event of a power failure, the SD card data is flushed at regular intervals; currently every second.

# Chapter 3: System Design

Through its development, the name Aries was chosen for VCU's new flight control system. The name was selected for the astrological symbol being VCU's official athletic moniker (Rams). This chapter will delve into the development process for the new autopilot platform and its various design considerations. It also includes the discussion of hardware fulfillment and component selection.

During the initial stages of development, the need for two separate platforms became apparent. The NextGen, while powerful, has come to a standstill due to the overly complex implementation. The emphasis of the NextGen was its ability to run complex control algorithms such as neural networks or other non-linear feedback controllers. At 200Hz, it utilizes less than 7% of the FCM and less than 20% of the ICM [22]. On the other hand, the miniFCS focused on a low cost and more disposable FCS for collaborative research. However, its slow processor, clocked at 33 MHz and lacking a hardware floating point unit, stunted the development potential of the miniFCS Thus the need for new hardware arose.

The Aries FCS solution comprises of two independent hardware platforms (Aries and Aries Tiny) to accommodate the applications of prior VCU FCSs. The Aries was made larger with more connectivity for on-board and off-board devices. The Aries Tiny, as the name implies, was made smaller and simpler with only the necessary circuitry for flight, with the exception of an on-board GPS.

## 3.1 System Requirements

The original design for the new autopilot initially targeted a replacement for the miniFCS and not the NextGen The desired dimensions for the new system should be similar to the miniFCS and it should meet or exceed the miniFCS feature set and peripheral connectivity. Additionally, a major addition was desired in the form of an on-board IMU solution, something not present on either the miniFCS or NextGen. Had the replacement of the NextGen been a higher priority, the architecture of the Aries platform would have been informed by that design instead. That said, the Aries can still be compared as a viable replacement for the NextGen at its current state. From the start of the project there were several fundamental constraints that remained in place throughout the project: a powerful microprocessor, a fully integrated sensor suite, low power consumption, and low overall cost.

The requirements for the microprocessor were straight forward: most important was a FPU, necessary for running the NextGen control loops at 50Hz while also running the complex sensor fusion algorithms developed in the UAV Lab in [25]. It also needed a high level of connectivity, including multiple timer capture compare channels, UARTs, I2C, and SPI. It needed the capability to run the NextGen control loop at 50Hz, while performing complex sensor fusion algorithms. This also includes processing other peripheral data such as analog, telecommunication, and navigation. Other restraints imposed also included IC packaging and availability.

Diverse external connectivity support was desired to accommodate current and future use. A minimum set of four servo PWM input and output channels (aileron, elevator, throttle, and rudder) were necessary. At least three external UARTs need to be made available (for external GPS, modem, and IMU) as well as one external I2C and SPI. These requirements were relaxed some for the Aries Tiny in order to retain the size restraint.

As noted in [8], barometric altitude measurements should have a range accurate to 1500 feet to the point at which GPS could be used for anything higher. Airspeed must be measurable to 200 knots with sub-knot precision. Both static and dynamic pressure sensors must be ported to allow for an external pitot tube, to combat potential pressure differentiation in the airframe.

The GPS unit should update its positional data at 10Hz. Its interface communication must support National Marine Electronics Association (NMEA) sentences. The module must include, at a minimum, the complete solutions for position, velocity, and time.

The embedded IMU solution must include tri-axis accelerometer, tri-axis gyroscope, and tri-axis magnetometer yielding 9-degrees of freedom. For precise tracking among high and low motion applications, the unit should also include user-programmable scaling sensitivity ranges. The IMU must allow for high speed communication with an output data rate greater than 1000Hz. This enables oversampling of data for applying software filters to alleviate noise.

The communication link must operate at frequencies other than 2.4GHz and not share harmonics within the spectrum. In previous generations of VCU UAVs, the limitation was imposed by the RC pilot's transmitter. Channel hoping and the use of different signaling methods may allow the RC and FCS radio to coexist on the same platform. However due to uncertainties, the FCS board must accommodate a radio operating outside the 2.4GHz band, while sharing the same form factor as a higher bandwidth 2.4GHz modem. This ensures some future compatibility in the case where a higher bandwidth becomes necessary. The modem requires enough throughput between the ground station to achieve vehicle state information updated at no less than 5Hz. As with the miniFCS, the modem must continue to support mesh networking for the continuation of collaborative UAV applications.

Safety switches allow the safety pilot to take control of the aircraft regardless of the FCS state. External installation often results in a mess of wiring and space, inhibiting the use of smaller airframes. The integration of the safety switch onto the Aries PCB was one of the largest requirements. It achieves a more compact solution and easier in-field setup.

The Aries size constraints should closely adhere to that of the miniFCS's targeted dimensions of a credit card. Keeping the PCB small in turn broadens its applications and selectable airframes. Weight concerns were never a large factor; by simply following the size constraints weight would be kept within reason .

## 3.2 Aries Design and Development

The Aries endured several iterations of hardware revisions before settling on a final design. Many of its design considerations were adopted from previous VCU UAV (miniFCS and NextGen), as previously mentioned. In total there were five board revisions: 0.1, 0.1.1, 0.2, 1.0, and 1.1. Versions 0.1 and 0.1.1 shared the same components and were nearly identical, with the exception of minor trace and routing alterations. TTo reduce confusion, both versions 0.1 and 0.1.1 will be referred to as "version 0.1" in the rest of this work. Versions 0.2, 1.0, and 1.1 were also very similar to one another. Power alterations and minor component integration set them apart from one another. The Aires Tiny received only two revisions (1.0 and 1.1), with the only alteration being an added console header. This section will overview the selected hardware components and circuitry of each Aries revision.

### 3.2.1 Processor

Early considerations included a multiprocessor architecture similar to the NextGen's solution. The design would allow separation between computationally heavy algorithms (for example FCS and IMU) from auxiliary sensor data processing. Several Digital Signal Processors (DSP) were evaluated for their double precision FPU and Fast Fourier Transform (FFT) implementation on chip. However due to packaging and cost, the use of a DSP was dismissed.

The use of an peripheral FPGA to alleviate sensor computation and other tasks from the main processor was also considered. It could also serve as the needed safety switch for the Aries. Extensive IO connectivity and hardware defined communication protocols provided by the FPGA would extend the Aries End-of-Life (EOL). Unfortunately, the added benefit was outweighed by many costly disadvantages. Over time FPGAs themselves can become difficult to obtain. Vendor support commitments are not always guaranteed causing device obsolescence. FPGAs typically draw large currents and require several different voltage supply levels, forcing a more complex board design. From a software perspective, it can also be difficult to maintain. The Synthesis tools are expensive and require frequent updates, which often leads to continual maintenance of the project.

Eventually, the design settled on a single core processor. The processor used in the Aries is the STM32F4, which is an ARM-based microcontroller created by ST Microelectronics. The STM32F4 is based on the ARM Cortex-M4F, which features a single-precision floating point unit [26]. The presence of an FPU was considered a must-have for the Aries in order to be able to run both FCS and IMU software effectively. The processor can be clocked at $168MHz$ with a High Speed External (HSE) oscillator. ST markets the STM32F4 as part of its "connectivity" line, as reflected in the high amount of IO options available for this processor, most of which are utilized in some fashion by the Aries. The device offers up to 17 timers, with between 1 and 4 channels available for each timer, as well as six USARTS, three SPI busses, and three I2C busses. It also offers integrated Ethernet MAC, SD card, and USB support.

There are several different lines within the STM32F4 family. Various packages are also available, ranging from small 64-pin devices to BGA devices having over 200 pins. Additionally, some features are not present across the entire line: the STM32F405/415 do not have any Ethernet support, while only the STM32F415/417 support hardware accelerated cryptography. There are also higher-end models which support additional types of external RAM. The Aries uses two versions of the STM32F4x7 processor: the Aries uses the STM32F407VG, a 100-pin LQFP package, and the Aries Tiny uses the STM32F417IG, a 201 pin BGA package.

The Aries, as the more full-featured of the two boards, exercises the full extent of the STM32F4's connectivity options. All available USARTS are in use, although due to the use of other peripherals, only 4 of the 6 USARTs are available. USARTs are used for the onboard modem and GPS, and a console, as well as having an extra USART for external peripherals. Only one SPI bus is made available due to pins sharing of other alternate functions. SPI communication is selected between on-board flash storage and future external peripherals. Despite having 3 I2C busses, due to hardware configuration only one I2C bus is available for the Aries, and this bus does the brunt of peripheral interfacing work. Both digital barometric sensors, the IMU sensors, and the safety switch processor all interface to the main processor over this I2C bus. The Aries also features an Ethernet PHY which enables ground communication over Ethernet, and a micro SD card to facilitate data logging and recovery. The USB support of the STM32F4 is wired up, and powering over USB is supported, but as of this writing there is no software support for Serial over USB or programming via USB.

The Aries Tiny, despite having many more connectivity options from the additional pins available on the BGA version, has far less actually in use due to the need to maintain a small form factor. All core peripheral connections are available, with the exception of external SPI. The Aries Tiny utilizes 4 USARTs: GPS, modem, console, and one external peripheral. Additionally, the Ethernet connectivity has been removed, but USB and microSD card connectivity were retained

Both Aries and Aries Tiny use the ADC of the STM32F4 line for battery voltage monitoring. Additionally, external ADC inputs, appropriately buffered, are available for external peripherals. Both boards also have support for the RTC of the STM32F4, and both contain a small coin-cell battery which will keep the RTC information valid for up to two weeks. On the Aries, this battery is also used by the on-board GPS to maintain fix data when powered off, which allows for a quicker reacquisition time after a power cycle.

As mentioned, some of the features of the STM32F4 are not in use in the final versions of the Aries and Aries Tiny. On version 0.2 and newer, the safety switch handles all servo control, so no external timer features are used. Although hardware support is present, the USB connector is effectively only used for power at this time.

### 3.2.2 Safety Switch

The Aries FCS solution incorporates a built in safety switch that allows the safety pilot to take full control over the aircraft at any moment. A microcontroller monitors a specified PWM input channel to switch output signals between the RC receiver and autopilot control. If the input signal has a pulse width lower than 1500 $\mu$s, manual mode is engaged; any pulse higher will switch to autonomous control. This threshold is configurable by software as desired.

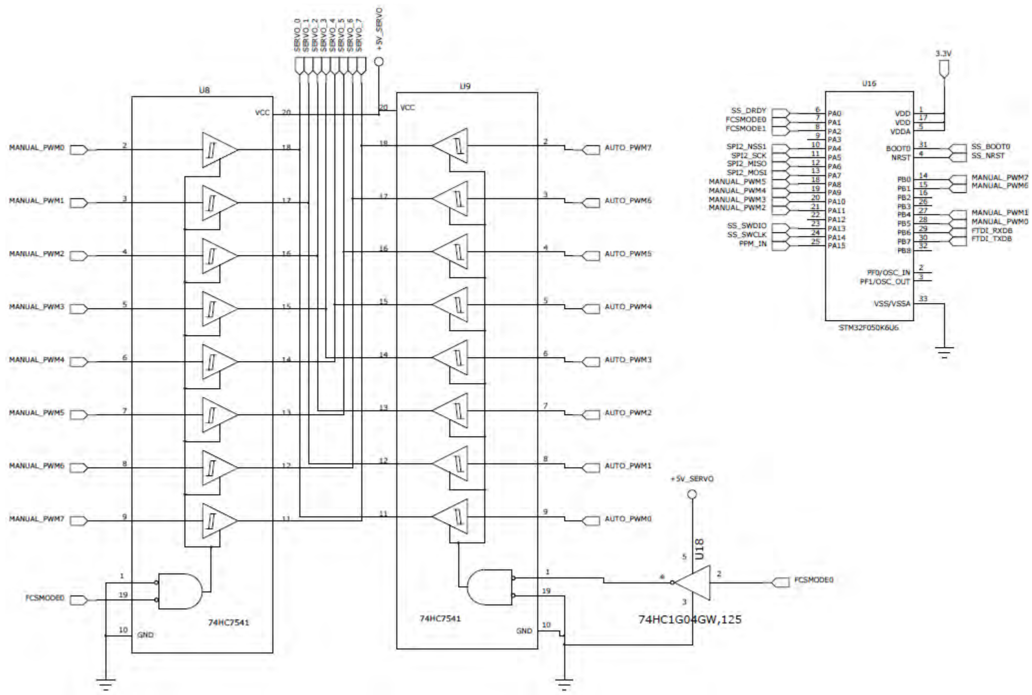


Figure 3.1: Safety Switch Schematic for Aries V0.1

There have been two versions of the safety switch. The initial Aries version (v0.1) used the STM32F030. Its circuitry, shown in Figure 3.1, followed similar switching architecture to the miniFCS [8]. Two eight port tri-state Schmitt trigger buffers (74HC7541) switched the output PWM channels between the RC receiver and the autopilot processor. An enable signal controls both buffers with the use of an inverter. The Schmitt triggers provided input channel hysteresis, increasing noise immunity for signaling servo control. This is useful when using noisy analog RC radios. An added benefit over the miniFCS was the ability to monitor all eight input channels, which was communicated to the main processor through SPI. This created the opportunity to dynamically change the monitor channel for auto/manual control, without the need to reprogram the safety switch.

When creating the final form factor of the Aries, a new safety switch control circuit was designed. Hysteresis inputs were no longer necessary, due to analog VHF transmitters being phased out for less noise prone digital 2.4GHz transmitters. Also, under the original schematic design, the Schmitt trigger buffer would not alleviate inadvertent switching on the RC auto/manual channel caused by noise. Therefore, the Schmitt triggered buffers were deemed unnecessary.

Version 0.2 and newer use the STM32F051. The STM32F051 features 6 externally-connected timers for a total of 15 channels, as well as two internal timers which can be used for software purposes. Between PWM in and out and PPM in, the Aries uses all 15 timer channels. The STM32F051 also has both SPI and I2C busses available. In order to utilize all 15 timer channels, it was necessary to use I2C. The processor also has two USARTs. One is pin-shared with PWM channels, and can be configured in software to be used for debugging purposes. The other is dedicated to Futaba S-BUS support.

Futaba S-BUS enables a series of servos to share the same signal line [27]. The proprietary protocol was reverse engineered among the open-source community [28]. This article describes how the protocol transmits with big endian, but individual bytes are transmitted as little endian. With the use of an $100kbps$ symbol rate inverted UART the Aries safety switch is capable of interfacing with Futaba S-BUS receivers. This dramatically reduces the complications with incorporating the FCS into the aircraft.

The safety switch on the Aries handles all servo input and output for the platform. The F051 offers additional timer channels which were unavailable on the F030, which enables the use of up to 15 timer channels for either PWM input, PWM output, or PPM input. The safety switch is capable of handling PWM input or output for standard 50Hz, 500 to 2500 $\mu$s pulse width PWM. The Aries supports both PPM input and Futaba S-BUS input in addition to traditional PWM input; this allows for the use of lower-cost receivers for manual flight. As configured for the Aries, it supports 7 inputs and 7 outputs, however the inputs can be oriented as outputs to achieve a total of 14 at which S-BUS would provide manual control.

The safety switch communicates with the main processor solely via I2C. All inputs, whether from S-BUS, PPM, or PWM capture, are captured in the safety switch and communicated over the I2C bus. The safety switch monitors the state of the auto/manual and failsafe channels as well. In auto mode, the values written by the processor are used, while in manual mode the values captured on the inputs are mirrored to the outputs. The safety switch makes use of a data ready pin which is asserted when one or more PWM channels have changed sufficiently (more than 3 $\mu$s) which allows the main processor to avoid polling the device. This is also used when the failsafe signals are detected. Two separate GPIO pins control a bi-color LED to serve as a visual for the auto/manual state. Red indicates manual operation, while green indicates autonomous mode. Future use could include an augmented state between auto and manual and be indicated as yellow.

The added connectivity to the safety switch processor increased the likelihood of overvoltage damage, since many pins are not $5V$ tolerant. Final versions (v1.0 and higher) of the Aries include direction controlled SN74LVC245A buffers to protect the safety switch if improperly connected. This has the added benefit of performing down voltage translation if ever $5V$ tolerance is necessary [29].

The Aries Tiny utilizes the same safety switch processor and is interfaced identically with the Aries. This lets both platforms be flashed with the same binary file. Only partial functionality is made available on the Aries Tiny. It has 7 PWM output channels, however all capture channels were omitted to maintain size constraints. Instead, RC input control is handled entirely through the Futaba S-BUS.

### 3.2.3 Power Supplies

Aries power management circuity and design went through numerous changes. Nearly every revision included power modifications. In total, there were three completely different designs that spanned across its development. Both switching and linear regulators and combinations of the two were tested for performance and accuracy. The Aries consists of two main power regulators operating at $5V$ and $3.3V$ respectively.

The Aries Tiny relies on external servo power for its $5V$ supply. It contains two linear regulators (a $3.3V$ for the digital network and a $3.3V$ for the analog network). This section overviews each design and its drawbacks.

### Aries Versions 0.1

Aries version 0.1 relied on two Texas Instruments (TPS5450 and LM2831) switching regulators to provide $5V$ and $3.3V$ respectively. The TPS5450 step-down device provided a large input voltage range of $5.5V$ to $36V$ allowing 8-cell lithium-ion polymer battery support [30]. TPS5450 is designed for continuous $5A$ current output with relatively small SMT inductors and capacitors though 500KHz PWM switching. Among other features, it includes: overtemperature shutdown, overvoltage protection, and overcurrent limiting. Given the TPS5450's large current source, the Aries could in turn distribute power to its connected servos without the need for an external Battery Equivalent Circuit (BEC). This benefit would only be seen on smaller aircraft, where actuating control surfaces does not draw significant current. Larger aircrafts would still require the separate source.

The LM2831 relied on the TPS5450 for input voltage, because of the lower input operating range ($3.0V$ to $5.5V$) [31]. Its $1.6MHz$ switching frequency reduced the required inductor and capacitor size, saving board area space, while delivering $1.5A$ current. The ability to source $1.5A$ was particularly alluring since majority of the Aries components are powered from $3.3V$. During its selection, the Aries was anticipated to only require $500mA$ for the entire board including peripherals. This provides significant room for future external devices, while still maintaining high efficiency with inconsiderable voltage drop.

A separate $3.3V$ linear power network for analog components was implemented to filter noise inherently introduced by the on-board switching regulators and digital circuitry. The circuit contained an ultra low noise Low-Dropout (LDO) Micrel MIC5219, featuring $500mA$ output rating [32]. As with the $3.3V$ digital power supply, the analog power regulator receives input from the $5.0V$ switching regulator. Anti-resonance and noise considerations required decoupling ferrite beads to the input supply and ground network. Low-Q beads were selected for their lossy characteristics and absorption of high frequency current noise [33]. The analog circuitry was retained throughout all revisions of the board including the Aries Tiny.

### Aries Versions 0.2 and 1.0

Despite following the recommended schematic and layout for the DC-DC switching regulators, version 0.1 voltage supplies delivered large transient noise that coupled to analog and other noise sensitive sensors. The purposed solution eliminated the use of step-down devices and relied solely on linear regulators. Versions 0.2 and 1.0 utilized STMicroeletronics L78 linear voltage regulator for its $5V$ power rail. The robust L78 offers an input range of short circuit and thermal overload protection [34]. With proper thermal sinking, the device offers up to an amp of power. The reduction in current output compared to the TPS5450 was an acceptable expense. Normally, the FCS does not need to provide power to the servos; each servo shares power with the safety pilot receiver, which is delivered by a either a BEC or an Electronic Speed Controller (ESC). The added benefit for powering the servos through the FCS was arguably unnecessary.

The $3.3V$ digital source was replaced by STMicroelectronics ST1L05, which provides a fixed output voltage and $1.3A$ current capability [35]. BiCMOS technology ensures no greater than $650uA$ quiescent current is maintained across all operating temperatures. The ST1L05 quickly stabilizes with small ESR ceramic capacitors, helping reduce the overall footprint of the circuit. This design was utilized in all the remaining Aries revisions, including the Aries Tiny.

### Aries Version 1.1

Heat dissipation became a primary problem with the strict use of linear voltage regulators. With all peripheral devices enabled, the Aries draws $450mA$. Under the assumption that a 3-cell LiPo battery ($12.6V$ input voltage and the absolute maximum safe input voltage) is used, equation 3.1 reveals nearly $3.42W$ of power dissipates into heat to provide $5V$ to the Aries circuitry. Version 1.0 attempted to mitigate the problem with a SMT heat sink. However, without proper airflow the heat sink cannot dissipate the thermal energy quickly enough under ambient temperatures. Concern for the longevity and accuracy of temperature sensitive components required another power solution.

$$Po = (Vi - Vo)/I \tag{3.1}$$

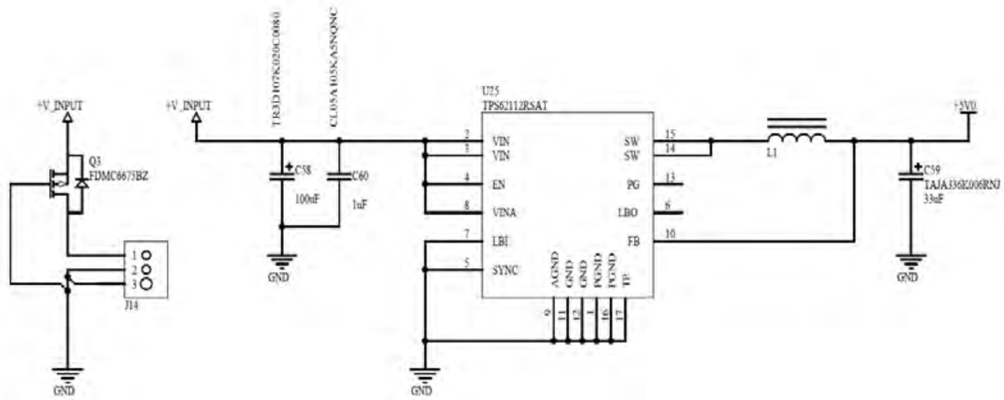


Figure 3.2: Aries Version 1.1 DC-DC Regulator Schematic

Aries version 1.1 ceased using the 5.0*V* linear voltage regulator and returned to a DC-DC switching regulator. The step down converter chosen was a Texas Instruments TPS62112, which offers significantly lower noise operation, with an input range of 3.1*V* to 17*V* and 1.5*A* output current [36]. This allows support for 2 to 4-cell LiPo battery without the concern to dissipate excessive heat. In the implemented configuration in Figure 3.2, the TPS62112 switches at 1.0MHz and enters an energy saving mode, when the load is under 200*mA*. Light current loads utilize Pulse Frequency Modulation (PFM), while heavy current loads revert to PWM, achieving 95% efficiency across the operating range. Synchronous rectification at 5*V* increases efficiency and reduces component count, helping accommodate the added circuitry footprint required for the DC-DC regulator. The device contains built-in overcurrent and overtemperature protection; reverse polarity protection is accomplished by a PMOS transistor shown in Figure 3.2.

### 3.2.4 RTC Battery Backup

Version 0.2 began the inclusion of an RTC battery backup circuit shown in Figure 3.3 for both the STM32F4 and on-board GPS module. The Schottky diode allows the battery to recharge when the board is provided power, but inhibits current flow in the opposite direction when not. The battery in use is a rechargeable Seiko Instruments 3*V*, 5.5*mAh* manganese silicon lithium battery. It can endure 100 discharge and charge cycles of 3.3*V* to 2.0*V*, as well as continued stable capacity after overdischarging to 0.0*V* [37]. Once given GPS fix data, the STM32F4's RTC will maintain

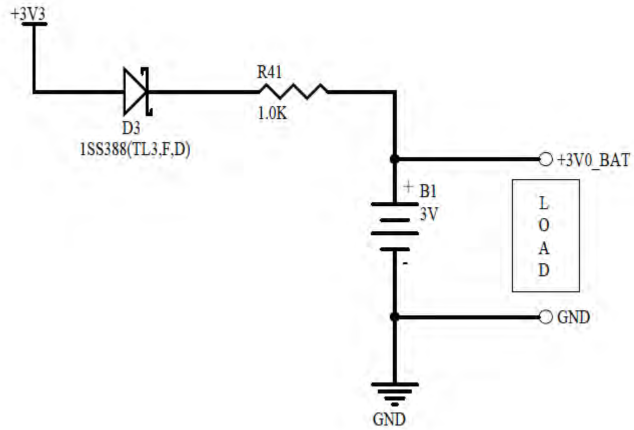


Figure 3.3: RTC Coin Battery Backup Schematic

accuracy even when powered off. This allows the FCS to retain the correct time for data logging well after the system has not reacquired GPS lock. Ephemeris data is also preserved enabling "hot starts" for the Aries on-board GPS.

The battery supplies the RTC and backup SRAM on the MCU and GPS module. Backup power consumption on the on-board GPS typically uses $7uA$ [38]. With RTC and backup SRAM on the MCU typically consumes $1.42uA$; with RTC and backup SRAM off the MCU typically consumes $0.10uA$ [26]. Noting the power consumption when RTC and backup SRAM are off is important because this state exists when the Aries has not been programmed with the FCS software.

Table 3.1: Estimated run time based off of current typical consumption on a $5.5mAh$ lithium battery

| FCS Platform | Current Draw | Run Time |
|---|---|---|
| Aries: Unflashed MCU | $7.1uA$ | 32.3 days |
| Aries: Flashed MCU | $8.42uA$ | 27.2 days |
| Aries Tiny: Unflashed MCU | $0.1uA$ | 2291.7 days |
| Aries Tiny: Flashed MCU | $1.42uA$ | 161.4 days |

Table 3.1 illustrates the estimated run time for both the Aries and Aries Tiny devices. It is a rough estimate that assumes the battery maintains a close $3V$ throughout the duration.

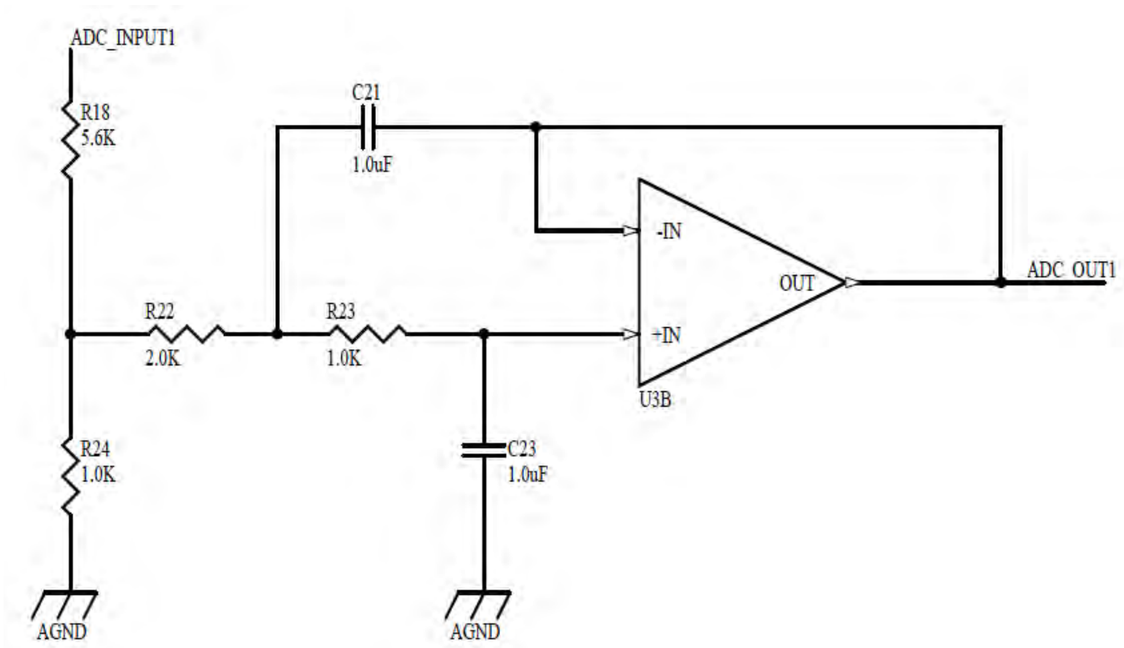


Figure 3.4: Aries low pass filter (112Hz cutoff)

### 3.2.5 Analog Signal Conditioning

Each Aries revision contained the same analog signal condition circuitry demonstrated on the miniFCS [8]. Each analog input uses a Sallen-Key low pass configuration, shown in Figure 3.4, designed to have a 3dB corner frequency at 112Hz. Maxim Integrated MAX9615 dual op-amp package were chosen for key characteristics: rail-to-rail output, low offset voltage, and low input voltage noise [39].

The low-pass filter attenuates a high frequency signal at 38dB demonstrated in Figure 3.5. $50mVpp$ noise will attenuate to $0.63mVpp$, which is slightly lower than the STM32F4's 12-bit ADC channel's $0.806mV$ per LSB. In practice, both Aries analog networks produce no greater than $30mVpp$ noise, which is completely filtered out.

To avoid clipping at the $3.3V$, a voltage divider precedes each low-pass filter to scale the incoming voltage. The Aries contains four ADC inputs: three external and one internal, which measures the boards power source. The Aries Tiny has a reduced number of ADC inputs: two external and one internal, utilized in the same manner. The Aries external ADCs are primarily used for bat-

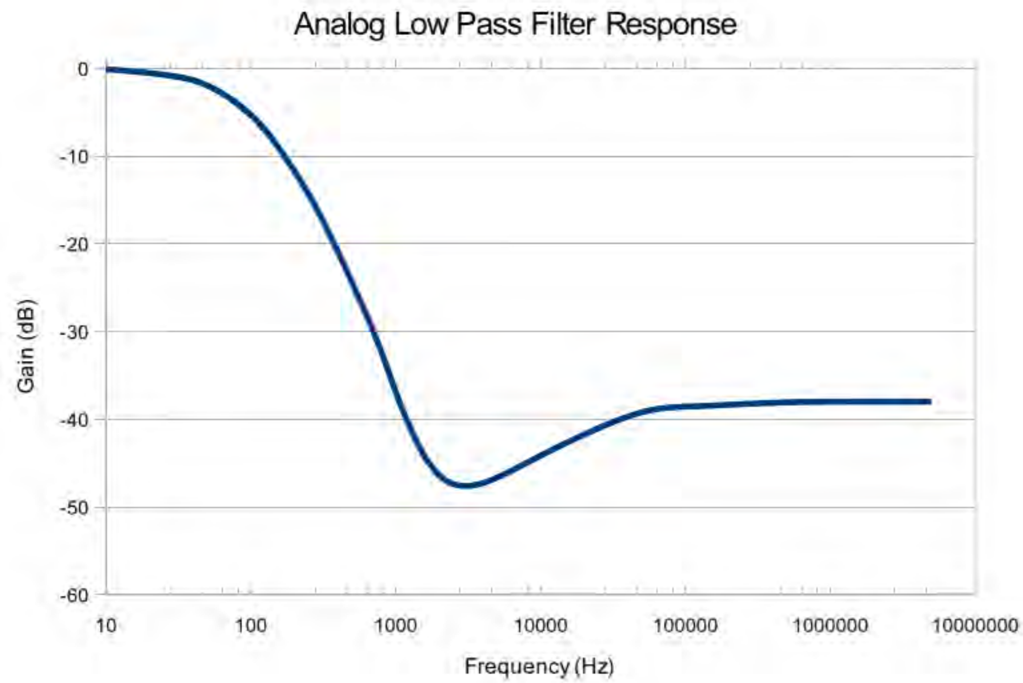


Figure 3.5: Analog low-pass filter response [8]

tery monitoring; one voltage divider supports a 12-cell LiPo, while the other two support only a 5-cell LiPo. Both external ADCs on the Aries Tiny support 5-cell LiPo. Neither configuration is permanent and can be adjusted by altering the voltage divider.

### 3.2.6 Barometric Pressure Sensors

Altitude and airspeed measurements are made available through static and differential barometric pressure transducers, respectively. Early Aries revisions implemented the same analog sensor configuration as the miniFCS. Both differential (model MP3V5004DP) and absolute (model MP3H6115A) pressure sensors were manufactured by Freescale Semiconductor. These sensors were chosen for their compact footprint and low cost.

The MP3V5004DP is temperature compensated between $10°C$ and $60°C$ and maintains $2.5\%$ accuracy over its operating range [40]. Pressure differential is calculated with the linear transfer function in Equation 3.2. Its operating range is between 0 to $0.568PSI$; with the STM32F4's on-chip 12-ADC, an accuracy of $1.39\times10^{-4}PSI$ per LSB is achieved.

$$V_{out} = V_s(0.2P + 0.2) \tag{3.2}$$

The MP3H6115A temperature compensates between -40°$C$ to 125°$C$, however it only guarantees 1.5% accuracy between 0°$C$ and 80°$C$ [41]. As with the miniFCS, the output was offset by -2.5361 and multiplied by 18.7 to bring greater altitude resolution between -50$m$ and 450$m$ [8]. To establish absolute pressure measurements the linear transfer function in Equation 3.3 is used.

$$V_{out} = V_s(0.009P + 0.095) \tag{3.3}$$

Complications with analog noise induced greater than expected inaccuracies for both altitude and airspeed calculations, motivating the decision to move to digital barometric pressure sensors. Aries version 0.2 began the inclusion of Measurement Specialties MS4525DO digital output transducers. The device features a 14-bit pressure output and an 11-bit temperature output, interfaced either through SPI or I2C, depending on the model [42]. Internal temperature compensation allows the device to operate with a Total Error Band (TEB)between -1 and +1% for temperatures -10°$C$ to +85°$C$. Extended error compensation between -25°$C$ to +105°$C$ is handled during data processing with an extended temperature multiplier table. The ceramic devices come in a variety of packaging (side port, top port, or manifold mount) for various measurement applications. Both absolute and differential packages utilized on the Aries were side ported for easy installation into the aircraft. The sensors also share the same transfer function shown in Equation 3.4; unfortunately, the sensor excludes 20% of its full 14-bit ADC range.

$$V_{out} = 80\% * 16383/(P_{max} - P_{min}) * (Pressure_{applied} - P_{min}) + 10\% * 16383 \tag{3.4}$$

The selected absolute pressure sensor is rated from 0 to 15$PSI$, with $1.14\times10^{-3}PSI$ per LSB. Unlike the miniFCS, the full pressure range can be utilized, allowing altitude readings well beyond 450 meters. The differential pressure sensor is rated from -1 to 1$PSI$, with $1.53\times10^{-4}PSI$ per LSB.

Its lower TEB allows for significant improvement over the MP3V5004DP.

### 3.2.7 Parameter Flash

Control parameter weights and other various data must be stored in non-volatile memory across flights and power cycles. The STM32F4 offers 4-Kbyte of backup EEPROM storage space [26]. The data is retained in standby mode with the presence of battery backup. Another option for application data retention is utilizing the extra space on the 1-Mbyte flash. However, any read/write operation halts all execution of code during that time. Both options were discarded in favor of an external EEPROM IC.

Microchip Technology's 25LC512 512-Kbit EEPROM was selected for various performance criteria [43]. Key features include: $20MHz$ clock speed, 1 million erase/write cycles, and $5ms$ 128-byte page write operations. Single byte write operations allow for quick control parameter tuning without the overhead of dumping the entire EEPROM page.

All Aries revisions include the 25LC512. It is powered from the digital $3.3V$ network and directly interfaces with the Aries SPI bus. A single $100nF$ bypass capacitor reduces transients during mode alterations. Read and write operations draw $6.33mA$ and $5.53mA$ respectively; releasing chip select, allows the device to enter standby mode and operate at $7.66uA$.

### 3.2.8 SD Card

All Aries revisions include a microSD card interface for data logging. The STM32F4 includes hardware Secure Digital Input/Output (SDIO) version 2.0 card compliance and supports transfer rates up to $48MHz$. The host controller enables Secure Digital High Capacity (SDHC) protocol supporting up to 32GB microSD cards.

The Aries utilizes SDIO in a 4-bit bus, offering significant performance improvement over single-bit SPI. Not all SD cards are guaranteed to support SPI mode, which would have limited compatibility. Card detection is made available on a hardware interrupt pin.

### 3.2.9 Ethernet

Hardware Ethernet support has been included through all Aries revisions, excluding the Aries Tiny. High bandwidth IP communication through the robust IEEE 802.3 architecture enables networking between other Aries boards and various auxiliary devices. Its inclusion should expand the usefulness of the Aries.

The chosen Physical Interface Device (PHY) was Texas Instrument's single port DP83848J transceiver [44]. The PHY connects the STM32F4's link layer to the Ethernet port via the 9 signal Reduced Media-Independent Interface (RMII). RMII utilizes half as many signal pins as Media-Independent Interface (MII), requiring an external $50MHz$ oscillator to accommodate the increased bus speed.

Auto crossover detection is handled directly by the PHY's on-chip auto-Medium Dependent Interface Crossover (MDI-X). The PHY's Built in Self Test (BIST) auto-negotiates 10 and $100Mb/s$ speeds. Auto-negotiation pin control is setup through strapping options. The chosen implementation enables both half and full duplex for 10BASE-T and 100BASE-TX.

The Aries board accommodates an on-board RJ45 Ethernet jack. The connector made by Pulse Electronics incorporates built in magnetics and green and yellow status LEDs [45]. The status LEDs are configured to indicate detected speed and link. $100Mb/s$ causes the assertion of the green LED; deassertion occurs through a link loss timer. Link presence asserts the yellow LED to blink during either transmit or receive activity.

### 3.2.10 USB

A Universal Serial Bus (USB) interface was included for all Aries and Aries Tiny revisions. It served to provide power and communication to the board for bench testing or affixing flight peripheral devices over USB.

Early USB implementation incorporated complex design decisions to provide greater functionality. Version 0.1 included a dual USB-Transistor-Transistor Logic (TTL) serial convert chip developed by Future Technology Devices International Ltd to allow communication for both the main processor and safety-switch over a single USB cable. The IC (FT2232D) required both a $6MHz$ external resonator and EEPROM [46]. Without the EEPROM, the device could not retain enumeration settings for requesting more than $100mA$. While the circuit proved successful, it offered very little benefit for the added complexity and footprint imposed on the Aries.

Aries version 0.2 offered a more elegant solution by directly utilizing the STM32F4's embedded USB On-The-Go (OTG) peripheral. While this removes the ability to communicate with the safety switch over USB, it does give the added benefit of the OTG specification. To refrain from over complexity an external PHY was omitted, disallowing USB 2.0. It was determined that USB 1.0 speeds would provide ample room for any communication required, since its primary goal was to provide system information console data.

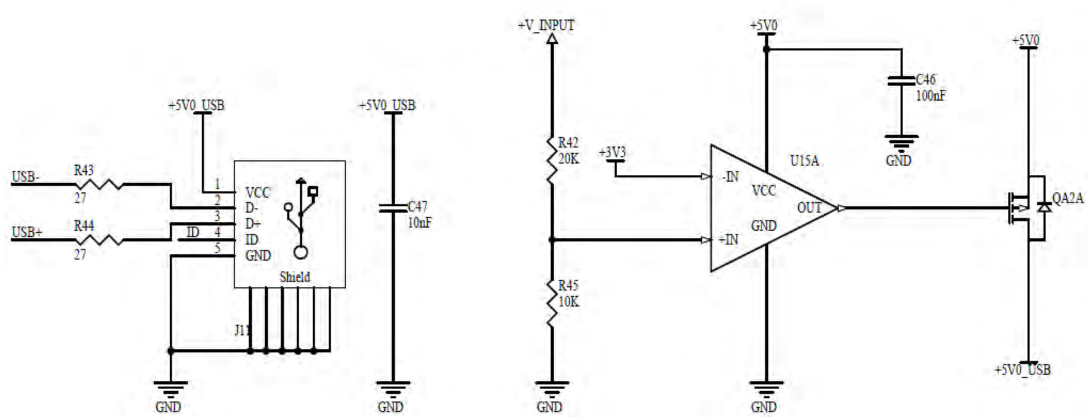


Figure 3.6: Aries USB power detection and selection circuity

To eliminate power sources from fighting one another, it was necessary to design circuitry for selecting the $5V$ power source, when a USB cable is plugged in. The solution in Figure 3.6, relies on an op-amp to drive the gate of the PMOS high at presence of "V_INPUT". In the absence of "V_INPUT", the gate is driven low and the PMOS turns on, powering the board with $5V$ USB power.

### 3.2.11 Inertial Measurement Unit

The initial Aries design included a 9-axis Micro-Electro-Mechanical System (MEMS) sensor, the InvenSense MPU-9150. It combines two dies into a single package device [47]. One die contains InvenSense's 3-axis accelerometer and 3-axis gyroscope; the other die is a third party 3-axis magnetometer by Akahi MicroDevices Corporation. The MPU-9150's biggest advantage was its I2C interface, which required less design accommodations required compared to other purely analog solutions.

During the Aries 0.2 revision design, the MPU-9150 was replaced by InvenSense's newer generation, MPU-9250. The magnetometer improves its full scale range four times over the MPU-9150 (from $1200uT$ to $4800uT$) as shown in Table 3.2. According to InvenSense, the gyroscope is three times more resilient to noise, although this is not represented within the datasheet. The accelerometer also improves and can output four times as fast. High output rates can be leveraged for software defined filters. The form factor was reduced by 44% from the MPU-9150, and more importantly a Quad Flat No-Lead (QFN) package was used as opposed to the Lead Grid Array (LGA) packing for the MPU-9150. LGA packaging recesses the leads underneath the device making it much more difficult to hand assemble and ensure proper connection. The QFN exposes the leads to the sidewall of the package, allowing visual confirmation the device is properly installed.

Sensitivity and scaling can be selected for varying uses of application. Dynamically changing the sensitivity could prove useful for different vehicle platforms with aggressive flight dynamics. Entering and exiting turns could be points where altering the performance of the MPU-9250 becomes advantageous.

### 3.2.12 Global Positioning System

The Aries 0.1 featured an integrated GPS with patch antenna. The FGPMMOPA6H by GlobalTop Technology Inc. provided a standalone package utilizing MediaTek's GPS Chipset MT3339 and built-in $15mm$ x $15mm$ x $2.5mm$ ceramic patch antenna [48]. The module could auto-switch

Table 3.2: Sensor characteristic comparison between MPU-9150 and MPU-9250

| | | Measurement Range | ADC Bit Resolution | Output Data Rate | Total RMS Noise |
|---|---|---|---|---|---|
| MPU-9150 | Gyroscope | ±250, ±500, ±1000, ±2000 | 16 | 4 to 8,000$Hz$ | 0.06 $°/s - rms$ |
| | Accelerometer | ±2$g$, ±4$g$, ±8$g$, ±16$g$ | 16 | 4 to 1,000$Hz$ | 4 $mg - rms$ |
| | Magnetometer | 1200$\mu T$ | 13 | 8$Hz$ | N/A |
| MPU-9250 | Gyroscope | ±250, ±500, ±1000, ±2000 | 16 | 4 to 8,000$Hz$ | 0.1 $°/s - rms$ |
| | Accelerometer | ±2$g$, ±4$g$, ±8$g$, ±16$g$ | 16 | 4 to 4,000$Hz$ | 8 $mg - rms$ |
| | Magnetometer | 4800$\mu T$ | 14 | 8$Hz$ | N/A |

between the Patch On Top (POT) antenna and an external antenna as well as detect and notify different antenna statuses, which encompassed active antenna, antenna shortage and antenna open circuit. The device supports 66 search channels with up to 22 simultaneous tracking channels. The output rate can be modified to 10$Hz$ with the Baud rate set to 115200.

While the FGPMMOPA6H's POT antenna enabled the Aries to obtain GPS fix without a costly external antenna, it was unable to maintain lock once inside the aircraft. This incident ultimately lead to the decision to move away from the FGPMMOPA6H and to Linx Technologies' RXM-GPS-FM-T for Aries versions 0.2 and up. This module includes the same MediaTek GPS Chipset MT3339 as the FGPMMOPA6H, but in a 23.8% reduced footprint.

The RXM-GPS-FM-T does not have a fix indication LED like the module used on 0.1; as such, a dedicated LED driver from the processor was added. This has the additional benefit of always providing GPS fix indication, even when an external GPS module is used.

With the inclusion of the RTC battery, the Aries system can utilize the entire feature set of the GPS module. The MT3339 chipset incorporated an embedded GPS assist system, which would calculate and predict satellite positions upon wake. Predicted ephemeris data can retained for up to 3 days. This enables "Hot Starts", which allow GPS lock in under 1 second. If a "Cold Start" is required, GPS lock should be obtained in under 30 seconds.

Since an external GPS system may be desired, the Aries included an external header that shared the same UART as the built-in GPS. Power to the built-in GPS is handled by a PMOS transistor so the device can be completely powered off when an external GPS is desired. To avoid the internal GPS from sinking signals on the UART even when powered off, it was necessary to add a tri-state buffer that was latched with the same GPIO driving the PMOS gate. When the GPIO pin is pulled high, the PMOS is turned off, turning the internal GPS off and isolating it away from the shared UART.

### 3.2.13 Radio Modem

Both Aries solutions have included an XBee modem for telemetry downlink. Since the Aries 0.2, the option has existed for either a through-hole or SMD XBee. With limited size, the Aries Tiny only includes support for a through-hole XBee.

Digi offers a wide range of models, which offer varying frequencies and features. The safety-pilot transmitter operates at $2.4GHz$ and due to safety concerns it is inadvisable for the FCS to operate at this frequency as well. The primary model used at VCU UAV lab is the XBee PRO 900HP series [49]. As the name suggests, it operates at $900MHz$. The data rate is capable of $200kbps$ and transmit power is software selectable up to $250mW$. It is capable of up to 4 miles range if line-of-sight is maintained. The supported network topologies include: DigiMesh, Repeater, Point-to-Point, Point-to-Multipoint, Peer-to-Peer.

In order to accommodate the SMD model, the Aries needed to allow the XBee to be programmed after it was installed as well as support an external modem. The solution included a Texas Instrument octal tri-state buffer (SN74LVC244ARGYR) [50]. The octal tri-state buffer contained two elements with 4 bits per element. The design allowed the TX, RX, CTS, and RTS signal pins to effectively connect together two of the three nodes (MCU, XBee, and external header). An external DIP switch drove the program enable single connecting the bus between the external header and XBee. By utilizing a PMOS transistor the internal XBee could be powered off. The signal driving the PMOS gate was also tied to a set elements tri-state buffer enable pin; turning off the XBee allowed the MCU to communicate with the external header.

The SMD XBee provides a fully integrated solution for incorporating an external antenna, which would allow the FCS to be fully enclosed. Also, since the modem is soldered directly to the board, connectivity loss from vibrations and jostled are effectively mitigated. Unfortunately, at the time of this writing, Digi only provides a $2.4GHz$ modem in this form factor. Therefore this feature was unable to be fully realized.

# Chapter 4: Printed Circuit Board Implementation

The Aries endured several iterations of hardware changes during its development. Most issues revolved around circuit alterations. If careful attentiveness to design geometries is not taken, performance issues can arise. This chapter overviews the precautions taken to ensure design issues did not present themselves.

## 4.1 PCB Design Practices

Many performance complications can present themselves through poor component layout and trace geometries. Particularly, the effects of transient currents and supply impedances are often overlooked. This section will overview some well known practices for board design optimization.

### 4.1.1 Board Stack Considerations

Multiple metal layers achieve high connectivity density, minimal crosstalk, and improve Electromagnetic Compatibility (EMC) [51]. These aspects facilitate optimal signal integrity between interconnecting components. Ideally, power and ground planes should separate signal layers from each other; they should encompass the full area of the board for best results. This reduces crosstalk, creates consistent transmission lines, and helps regulate characteristic impedance. In cases where dedicated ground and power planes are not possible, special care must be taken to avoid poor performance.

Ground planes do not guarantee a current signal will follow the best return path. Good board stack up designs must consider the power supply and ground references for a given signal. Adjacent layers above and below the signal layer should reference ground and power. Poor return paths harmfully affect signal references, causing a localized "bounce" [51]. This result can also negatively impact adjacent signals.

Vias typically provide two important functions: connecting through-hole devices to the board and joining traces together from different layers. The properties of a via are generally modeled as parasitic capacitance and inductance. A small diameter via has lower capacitance, while a larger via has lower inductance. These parasitic qualities can cause unforeseen complications. However, the imposed inductance is more commonly the culprit of problems through series impedance. High transient current supplies should be placed on upper layers closer to the respective component, minimizing the vertical distance through vias.

### 4.1.2 Decoupling Considerations

Insufficient decoupling capacitor sizing and placement can cause adverse effects on device performance [52]. Short, wide traces should be used to reduce impedance. A common source of noise usually relates to switching power supplies as well as high speed ICs. These cause rapid edge rates leading to fluctuating voltage swings. Decoupling capacitors function as a local power supply delivering short bursts, while not producing an additional noise.

Decoupling capacitor selection should not only be determined by an individual capacitance value. Parasitic characteristics such as Effective Series Resistance (ESR) and Effective Series Inductance (ESL) must also be taken into consideration [51]. All capacitors maintain their effective decoupling properties at specific frequency band. The size and geometry play a large role in characterizing its ESR and ESL. Tantalum capacitors generally have a wider effective band than ceramic capacitors, but are often much larger for their equivalent capacitance. X5R and X7R ceramic chip packaging yield lower ESR and ESL, however they exhibit a narrower effective frequency. To encompass a large effective decoupling band, an assortment of ceramic and tantalum capacitors should be used.

### 4.1.3 Localized Isolation

A board design mixing high frequency switching and analog circuitry must incorporate localized isolation [51]. Passive filtering through in-series ferrite beads serve to mitigate transients and noise. Large impedance from the source to the load can cause current noise translating into voltage noise seen from the load. It is important to minimize impedance while still correctly isolating the filtered network from the determined frequency. However, large bypass capacitors can be used to lower the imposed impedance.

## 4.2 PCB Design Implementation

Both Aries solutions took similar design approaches in terms of placement and isolation. The Aries STM32F4 used the 100-pin LQFP package, and the Aries Tiny uses the STM32F417IG, a 201-ball BGA package. Advanced Circuits was the manufacturer for the Aries PCB boards. They offer varying capabilities depending on the required specification, shown in Table 4.1. Further capabilities, such as smaller line spacing, microvias, and buried vias, require IPC Class 2 and lower. For practical reasons, the Aries PCB designs were limited to the $66 4-layer special.

Special care was taken to avoid via-in-pad as much as possible. Since the $66 special does not include epoxy resin via fillings, these holes will remain open. During the soldering process it is not unlikely that air-pockets will be created within the via hole. If the air expands, such as at high altitude or at high temperatures, the copper contacts could break away and disconnect the device from the trace.

Table 4.1: Advanced Circuits manufacturing capabilities

| Feature | $66 Special | Standard | Custom IPC Class 3 |
|---:|---:|---:|---:|
| Line Width | 6*mil* | 5*mil* | 4*mil* |
| Space Width | 6*mil* | 5*mil* | 4*mil* |
| Drill Size | 15*mil* | 10*mil* | 4*mil* |
| Annular Ring | 7*mil* | 5*mil* | 5*mil* |

### 4.2.1 Aries Board Design

The initial Aries designs were done with Mentor Graphics PADS. Version 0.1 was initially designed as a prototyping board to allow the Aries software to be developed simultaneously. This version shown in Figure 4.1 was intended to be sized and laid out similarly to the final version. Due to timing constraints, the board size was increased and the components manually placed to allow most of the signal nets to be auto-routed. Final dimensions for this version were 4*inch* by 4*inch*.

The only routing and geometry patterns done manually were on the power supplies. The switching regulators are most sensitive to trace layout and placement. These components were placed and routed according to their respective datasheets. The inductor needed to be as close to the switching node to prevent excessive capacitive coupling. Vias needed to be placed directly under the IC to connect to internal grounding planes. The output current loop area was minimized by placing the catch diode as close to the device as possible. Output capacitors maintained the current loop created by the switching node and inductor.

The Aries v0.2, shown in Figure 4.2, was the first revision designed with Altium Designer. Altium provided significant improvement over Mentor Graphics PADS. The software provided better organization of schematics and libraries. It also enabled via stitching which provided better references to ground on each layer. This effectively creates a stronger vertical connection through board layers creating shorter return paths and maintaining low impedance.

This design was completely manually routed in hopes to mitigate crosstalk and achieve the desired board dimensions (1.95*inch* by 3.5*inch*). The analog network was isolated from the digital

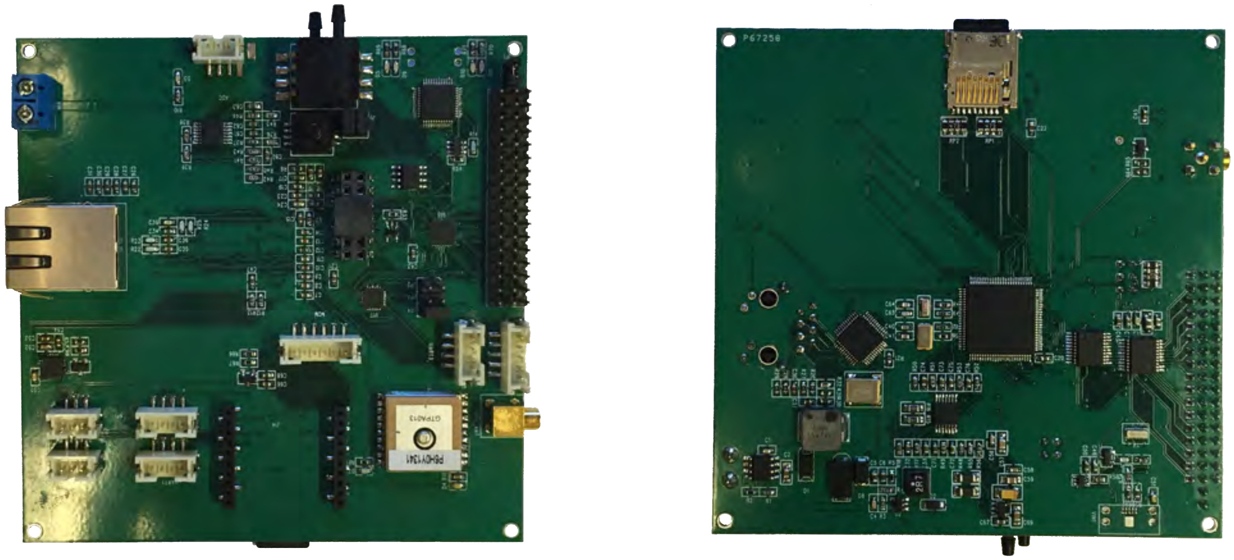

Figure 4.1: Aries v0.1 (top side on the left and bottom side on the right)

network by the use of separate grounding planes with ferrite beads bridging power and ground references. Wide, short traces were used to connect both the XBee and GPS modules to MCX antenna connectors to reduce impedance mismatching. These traces were also surrounded by copper poured grounding planes with via stitching for improved isolation between neighboring digital components.

Final revisions of the Aries design included mounting tabs that could be cut if deemed unnecessary in future use. However, their inclusion allows the board to be easily mounted to the airframe. Its dimensions are 2.65*inch* by 3.5*inch* with the added mounting tabs. The final version of the Aries is shown in Figure 4.3. Version 1.0 and 1.1 share an identical physical footprint. Both boards had similar routing strategies. An orthogonal routing strategy helped with signal integrity and minimization of crosstalk. Their differences in routing were largely the power circuit modifications.

Aries 1.0 required a SMD heat sink to dissipate the heat generated from the linear voltage regulator. Multiple vias surrounded the heatsink to allow it to dissipate over a larger area of the board. With the lack of airflow, the heat was not effectively mitigated. The result forced the design

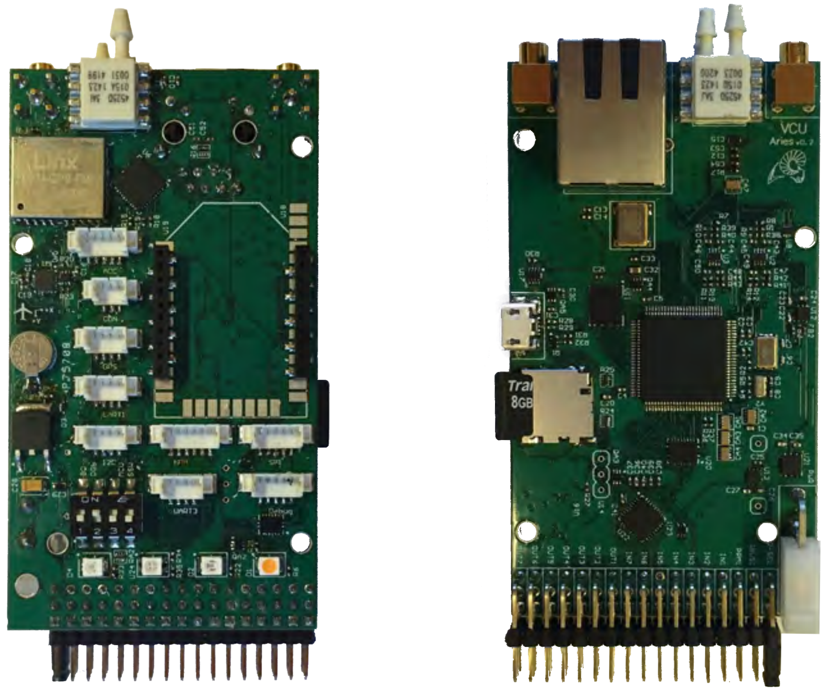

Figure 4.2: Aries v0.2 (top side on the left and bottom side on the right)

of version 1.1 to use a switching regulator.

Version 1.1 greatly reduced the heat profile compared to previous versions. The same design strategies for the switching regulator were followed with version 0.1. The higher switching frequency of the TPS62112 allowed smaller effective components. However, to achieve acceptable performance larger inductor and capacitor values than indicated in the datasheet were required.

### 4.2.2 Aries Tiny Board Design

The Aries Tiny was significantly smaller in physical layout. Its dimensions were 1.5*inch* by 3.2*inch*, which is a 48.2% reduction compared to the final version of the Aries. A balance between interfacing and size played a large role in determining its final dimensions. The final design is shown in Figure 4.4.

To test whether the VCU UAV lab could successfully install a BGA package, the Aries Tiny utilized the 201 pin UFBGA package with 0.65*mm* pitch. This had the advantage of 40.1% foot-

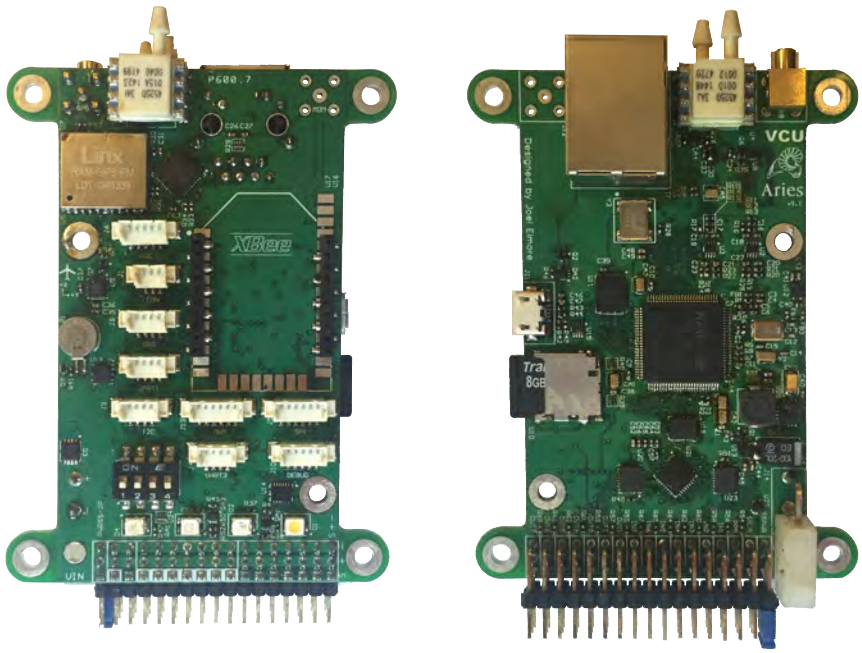


Figure 4.3: Aries v1.1 (top side on the left and bottom side on the right)

print reduction over the 100-pin LQFP package. It contained 176 balls on the outer edges and a square of 25 grounding balls in the center. Each ball measured an 0.28*mm* diameter.

The recommended layout included 0.3*mm* diameter pads and and 0.4*mm* diameter solder mask relief. Advance Circuits requires no smaller than 6*mil* or 0.1524*mm* for trace width and clearance spacing. In order to route a 0.152*mm* trace between two geometries, they must be no closer than 0.4572*mm* apart. With 0.65*mm* ball pitch and 0.3*mm* pad diameters, only 0.35*mm* of clearance is alloted. To work around this dilemma, the ball pads were reduced to 0.1778*mm*, which gives a clearance of 0.4722*mm*. Figure 4.5 shows how the Aries Tiny was laid out; the outer edged balls of the device are heavily utilized contrary to the inner balls.

The solder mask relief diameter was maintained at the recommended size as per the datasheet. Reliable industry studies highly recommend Non Solder Mask Defined (NSMD) pads over Solder Mask Defined (SMD) pads [9]. Figure 4.6 demonstrates the difference between the two. NSMD achieves tighter copper dimensions and reduces stress at the solder joint and top of the pad. The technique also provides improved uniform coverage over the pad. The exposed surface area on the side creates a tighter "grip" between the solder and the pad.

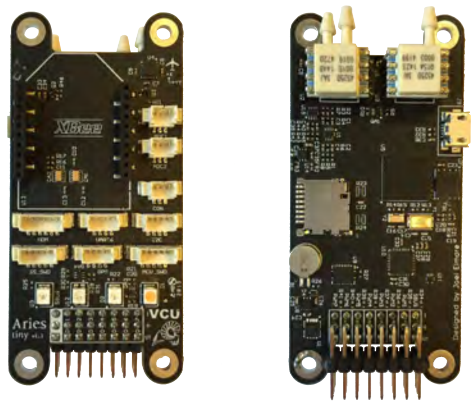

Figure 4.4: Aries Tiny (top side on the left and bottom side on the right)

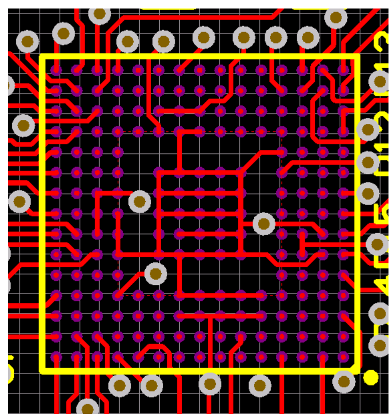

Figure 4.5: Aries Tiny STM32F4 UFBGA routing

Because of the clearance issues imposed on the Aries Tiny design by the $66 special, only the outer two ball layers could be used along with a few balls on the inner layers. The space between the signal balls and the grounding balls allowed for some vias to be placed underneath the device. The clearance problem required strict board planning and layout. Peripheral cores mapped to balls on the outer edges were placed at a higher priority. Any circuitry requiring an arbitrary GPIO or special functioning core were given the closest outer connections on the device.

Via placement is important. If the via is too close to the ball, the solder will be wicked away and connection between the pad and device will be lost. Soldermask helps reduce this effect by impeding the solder from traveling down the trace into the via. Unfortunately, via placement is not an option for connecting this specific BGA device under the $66 special, because of clearance

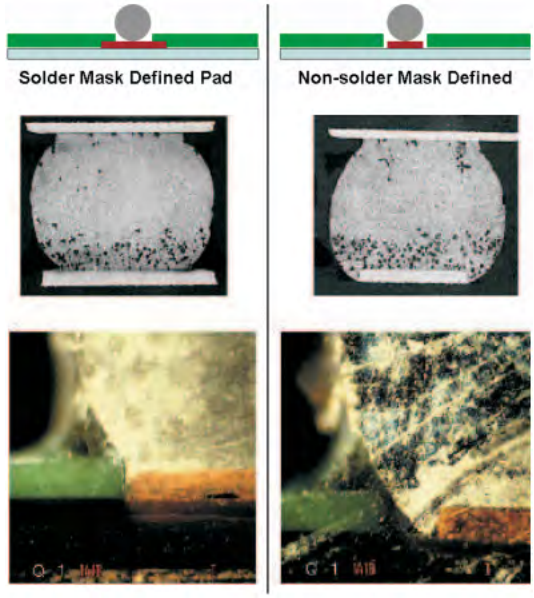


Figure 4.6: SMD pad (left) NSMD pad (right) [9]

issues. The smallest via size allowed is 0.7366*mm*. Advanced Circuits custom specification must be utilized in order for to implement vias in the appropriate size.

A more conventional method of BGA routing utilizes adjacent vias for each ball. This strategy is not be possible with the 0.65*m* pitch UFBGA package even under Advanced Circuits custom IPC Class III guidelines and with the reduced pad diameter. For this to be possible, a more advanced specification is required. Under Advanced Circuits custom IPC Class II guidelines, they offer 3*mil* laser drilled micro vias with 2*mil* annular ring.

# Chapter 5: System Evaluation

Each revision of the Aries underwent extensive testing to ensure it was safe for flight testing. HILS simulations confirmed various aspects of the flight control system were correctly operating. These tests helped evaluate the flight control platform without the risk of in flight failure. This chapter will demonstrate the overall performance and characterization of the Aries FCS.

## 5.1 Analog Performance

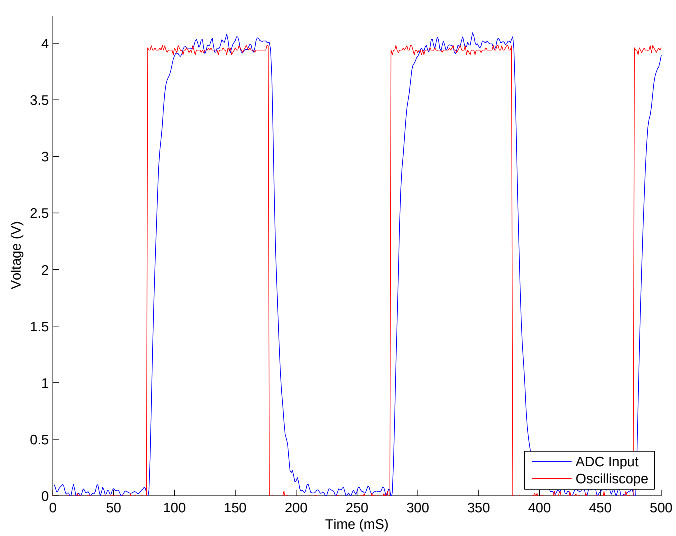


Figure 5.1: Aries Version 1.1 ADC step response

The analog stage of the Aries significantly improved since its first revision. A function generator was attached to an analog input channel of the Aries to test its step response, as shown in Figure 5.1. It demonstrated the response time of a sharp change which in most situations on the

FCS would be fairly rare. The ADC reading settles under $25ms$, from a $0.0V$ to $4.0V$ step.

## 5.2 Voltage Regulator Heat

After moving to linear voltage regulators, the Aries heat profile drastically increased. Figure 5.2 is a thermal image of the Aries version 1.0. A thermocouple revealed it reached $151.2°F$ at its hottest location (the $5V$ linear regulator). It is important to note the heat sink drawing heat away from the board and dissipating it on its side fins. Early thermal measurements taken of Aries version 0.2 reached $160°F$. The heat sink did provide some cooling at ambient temperature, unfortunately under static conditions it could not pull enough heat away from the PCB.

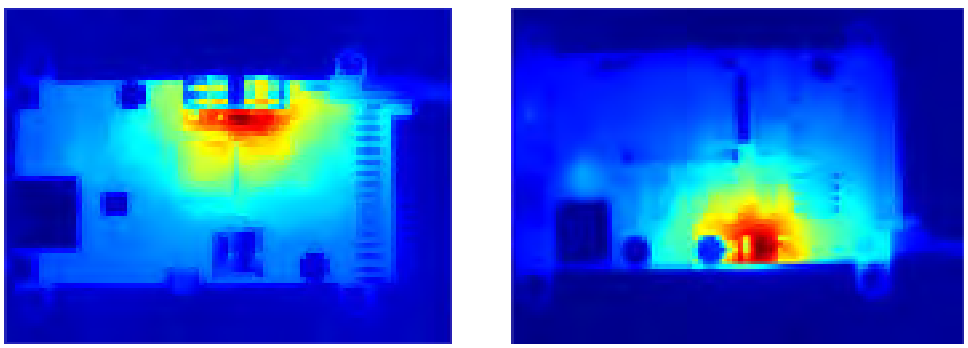

Figure 5.2: Aries version 1.0 thermal profile with $151.2°F$ at hottest point (bottom side on left, top side on right)

The heat profile of Aries version 1.1 shown in Figure 5.3 demonstrates significant improvement over previous linear regulator versions of the Aries. The hottest point reached $120.6°F$, which was seen on the $3.3V$ linear regulator. Figure 5.3 allows for other heat details to be seen since the thermal sensor is not being blown out. The MCU and the PHY intrinsically radiate a nontrivial amount of heat.

## 5.3 Platform Overview

Table 5.1 overviews several hardware details defining each platforms capabilities. While the Aries does not offer the same processing performance as the NextGen, it does improve on size

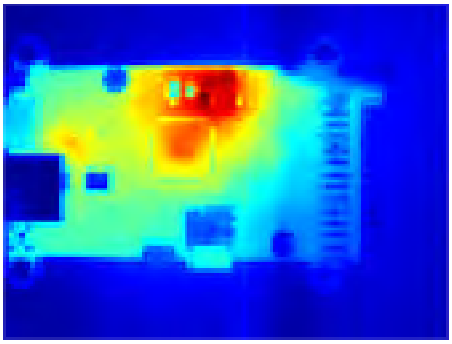

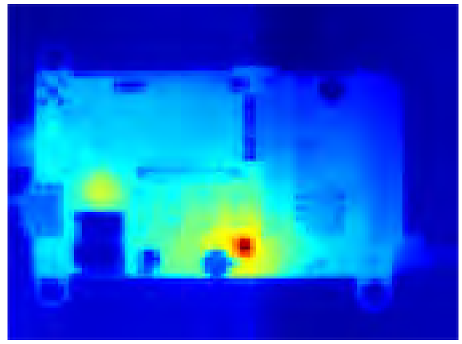

Figure 5.3: Aries version 1.1 thermal profile with 120.6°$F$ at hottest point (bottom side on left, top side on right)

and supported peripheral interfaces. Improvement over the miniFCS was seen in processor performance and peripheral support. Non-Volatile Memory (NVM) used for FCS related parameter gains is one area most platforms lack. With the integration of an external EEPROM, the Aries NVM is able to retain over 16,000 32-bit words. One of the key advantages realized on the Aries platform was its successful implementation of an on-board Ethernet interface. While the NextGen also achieved this, the Aries did so in a much smaller form factor at a fraction of the cost.

Table 5.1: Hardware comparison between notable FCS platforms

| | NextGen | MiniFCS | Aries | Aries Tiny | KroozSD | Pixhawk |
|---|---|---|---|---|---|---|
| Speed (MHz) | 200 | 66 | 168 | 168 | 168 | 168 |
| Dhrystone MIPS | 300 | 91 | 210 | 210 | 210 | 225 |
| Non-volatile memory | 64KB | 512Bytes | 64KB | 64KB | 0 | 8KB |
| Safety-Switch | Yes | Yes | Yes | Yes | No | Yes |
| RTC | No | No | Yes | Yes | No | Yes |
| GPS | Yes | No | Yes | No | No | No |
| Modem | Yes | Yes | Yes | Yes | Yes | No |
| Ethernet | Yes | No | Yes | No | No | No |
| UART | 6 | 4 | 4 | 3 | 3 | 5 |
| SPI | 0 | 0 | 1 | 0 | 1 | 1 |
| I2C | 0 | 0 | 1 | 1 | 2 | 1 |
| Size | 3.8 x 2.9 | 3.2 x 1.8 | 3.5 x 2.65 | 3.2 x 1.5 | 1.97 x 1.97 | 3.2 x 2.0 |

Table 5.2 provides peak-to-peak voltage noise seen on the power networks of the Aries revisions. The noise present on v0.1 is the worst of the others being compared. The Aries v0.2 contains the least amount of noise of all the compared platforms. As expected, the linear regulators provided

the best noise rejection performance. The Apogee was also included in the comparison, because it uses the same TPS6211 voltage regulator as the Aries v1.1. As shown in Table 5.2, the 3.3V power network has roughly 40mV less noise. However, this is not a truly fair comparison, as the Apogee draws close to 50mA and the Aries roughly draws 450mA. At nearly 10 times the load, the Aries performs better through careful routing design and technique. The Apogee does not have a separate low-noise linear regulator for its analog stage and instead shares power with the digital 3.3V network. The digital 3.3V network has nearly twice as much noise as compared to analog network on the Aries v1.1. Any analog measurements on the Apogee will reflect this noise.

Table 5.2: Comparison of peak-to-peak voltage noise on various FCS platforms

| | Aries v0.1 | Aries v0.2 | Aries v1.1 | Aries Tiny | Apogee |
|---|---|---|---|---|---|
| Input Power (mV) | 1028.0 | 38.9 | 546.5 | 123.5 | 649.5 |
| 5.0V Digital (mV) | 345.7 | 29.9 | 189.9 | N/A | 204.7 |
| 3.3V Digital (mV) | 354.3 | 27.9 | 168.3 | 113.7 | 207.0 |
| 3.3V Analog (mV) | 271.6 | 26.2 | 105.0 | 112.2 | N/A |

At the time of this writing, a complete cost evaluation of the Aries has not been performed. The Aries Tiny has gone through the entire fabrication procedure with a full cost analysis. Table 5.3 breaks down the cost for a set of 5 and 10 boards. The component cost of the Aries Tiny represents everything needed to make a complete board for fabrication. To be flight ready, the Tiny still needs an external GPS module ($35.96) and a XBee ($39.00). Since these modules are accessories and are unlikely to be purchased at the time of manufacturing, they have been excluded from the overall cost. In a quantity of 10, a flight ready Aries Tiny comes out to be $435.82 without taxes and shipping costs.

A full Aries will see similar pricing. The fabrication and board assembly will be fairly close to the Aries Tiny. The component cost is the only likely variation.

Table 5.3: Aries Tiny Manufacturing Cost

| Quantity | 5 | 10 |
|---|---|---|
| Components | $775.46 | $1481.42 |
| Board Fabrication | $656.30 | $701.10 |
| Board Assembly | $1,277.35 | $1,426.10 |
| Total Cost | $2,709.11 | $3,608.62 |
| Cost Per Board | $541.82 | $360.86 |

## 5.4 Flight Test Results

The flight tests were taken with a Red Dragonfly RC aircraft. It has a 900$mm$ wingspan and weighs approximately 514$g$ or 1.14$Lb$ with a 2100$mAh$ LiPo and complete Aries Tiny FCS. The data is gathered from the ground control system software which receives telemetry data at 5$Hz$. This data represents the FCS achieving its fundamental goal of providing a functional controller for UAVs.

### 5.4.1 Flightpath Tracking

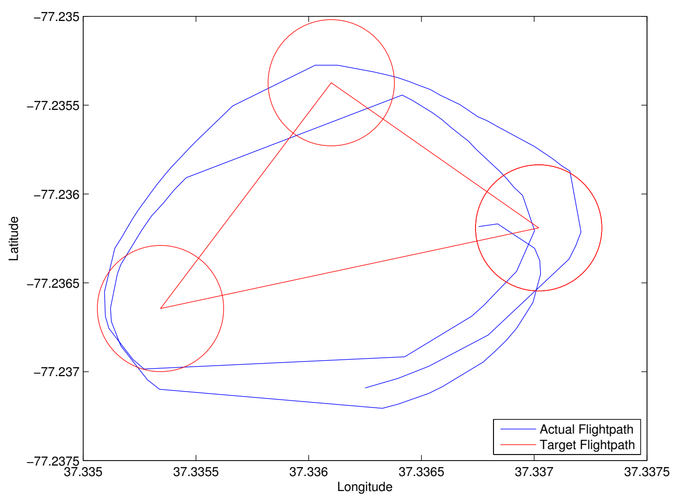


Figure 5.4: Aries Tiny GPS flightpath on the Red Dragonfly RC aircraft

Figure 5.4 represents an actual flight of the Aries Tiny. The flight control system was in a simple point to point navigation setting instead of following the Rhumb line. The longest leg on the figure is roughly $625ft$. The shown flight operated with an "arrival range" of $150ft$ (a radial diameter around each waypoint at which the aircraft considers to have arrived). Its size and weight causes the aircraft to get blown around. However despite its size, the FCS is able to accurately navigate the waypoints.

### 5.4.2 Altitude Hold

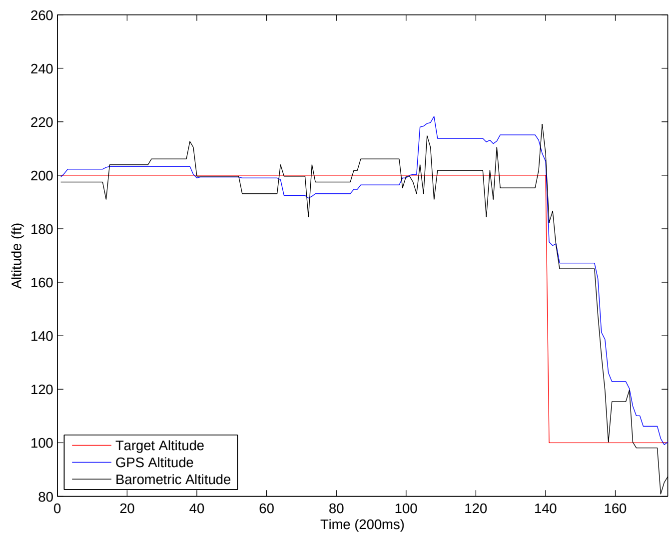


Figure 5.5: Aries Tiny GPS and barometric altitude measurements on the Red Dragonfly RC aircraft

Figure 5.5 demonstrates the altitude hold functionality of the FCS. Both the GPS and barometric altitude sensors are represented on the figure. The figure shows the FCS at a target altitude of $200ft$ then descending to $100ft$. A large variance between the two sensors exists. They do have an overall trend in which they follow, and it is difficult to determine which of the two is more accurate. At the current time of this writing, the FCS software does not include any software filtering that existed on the NextGen such as the altitude alpha-beta filter. The lack of any signal conditioning is likely why there are such large peaks and valleys shown on the graph.

# Chapter 6: Conclusions and Future Work

## 6.1 Conclusion

The Aries FCS solution demonstrates significant improvement over previous VCU UAV generations. It offers many of the functional benefits the NextGen provided, but under similar miniFCS implementation guidelines. The balance achieves proficient performance and maintainability at a competitive cost.

The Aries challenges what can be possible within the VCU UAV lab. Successful installation of BGA, 0402, and 0.40*mm* pitch devices illustrates the possibilities for the next generation of VCU autopilot.

## 6.2 Future Work

While the Aries system accomplished its targeted goals, it falls short in many areas. As a research platform, it should reduce friction of future development and incorporate a much larger ability for customization.

### 6.2.1 Hardware Connectivity

The Aries and Aries Tiny make several external options available. They include common interfaces that most external sensors would require. Unfortunately, neither boards made use of a backplane connector that would allow for various daughter boards to extend the future functionality. The NextGen designed a similar feature, where the auxiliary sensor board could be redesigned and updated more frequently. This concept was never taken advantage of, partially due to lack of necessity and partially due to potential complications with new integrations. With the strive for software modularity in Aries/RT and ChibiOS implementation, new hardware should be much easier to adopt than any previous version of VCU FCS.

### 6.2.2 Programming Method

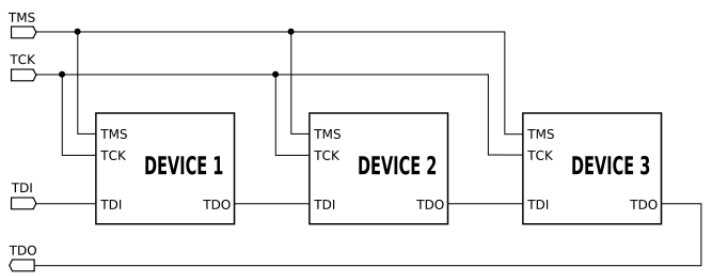


Figure 6.1: Daisy-chained JTAG topology (Test reset pin is not shown) [10]

Currently, both Aries boards are programmed through SWD, but have different accessibility. The Aries utilizes a MUX and DIP switch to offer a single header solution for programming the main processor and safety-switch. The Aries Tiny removes the complexity and separate programming headers are made available for each processors. In hindsight, both solutions were non-optimal. JTAG chaining in Figure 6.1 solves the problem of multiple processor programming through a single header. Doing so would remove the complexity of the MUX on the Aries and remove the added header on the Aries Tiny.

In order to program the Aries, it requires an ST-Link programmer. While this is not necessarily a large problem, it does add an extra step and device needed for development and in-field programming. A notable alternative is a small open-source programming circuit known as the Black Magic Probe [53]. This circuit would take full advantage of the on-board USB interface and provide programming for both the main processor and safety-switch with a single Micro-USB cable. With the incorporation of JTAG chaining, minimal footprint and cost would be required.

### 6.2.3 Board Architecture

It is worth noting the increased improvement and availability of SoC devices marketed towards mobile use. The Raspberry Pi and various other platforms achieve great performance at a price point simply unavailable before their inception. Even the first version (released February 2012) of the Raspberry Pi, clocked at 700MHz, offers over 4 times the clock speed of the STM32F4 processor. The second generation Raspberry Pi replaced the original version in February 2015 [54]. It features a Broadcom BCM2836 quad-core Arm-Cortex 7 $900MHz$ processor with $1GB$ of RAM.

It may be advantageous for future FCSs to take advantage of existing platforms like the Raspberry Pi 2 and design a daughter board instead. This would significantly reduce development costs, while still allowing full customization of sensor suites. An STM32F4 or similar micro-processor could be placed on the daughter board to run rudimentary flight control algorithms allowing independence from the Pi, but also allowing the option to piggyback the Pi's processor for calculation intensive applications.

A further step forward is to develop a fully integrated SoC solution. Advancing to an SoC would most likely require signing a Non-Disclosure Agreement (NDA). However, this should not be a problem for the VCU UAV lab which has no intention of making its FCS open-source. On the other hand, this poses significant challenges from both a hardware and software perspective. Not only would the hardware design require intricate and complex circuit designs, the manufacturing processes necessary to fully accommodate a pin-dense BGA would most likely require buried and blind vias. The advanced manufacturing processes immediately rules out any cheap one-off builds. Instead similar costs to the Aries final production would be required multiple times during development. It is arguable, however, the extra time and development cost would increase the lifespan of the FCS and make it more cost effective in the longterm.

The software would require a complete overhaul from the original Aries solution. A migration to a Linux based architecture would be the most beneficial. If done similarly to the Aries modular drivers, the new system would yield future proofing and ease of adoption of new peripheral and entirely new FCS hardware.

# Bibliography


[1] (2014, March). [Online]. Available: http://wiki.paparazziuav.org/wiki/KroozSD

[2] [Online]. Available: http://wiki.paparazziuav.org/wiki/Apogee/v1.00

[3] [Online]. Available: http://pixhawk.org/

[4] [Online]. Available: http://www.cloudcaptech.com/piccolo_system.shtm

[5] (2015) Kestrel flight systems: Fly light with kestrel onboard. [Online]. Available: http://www.lockheedmartin.com/content/dam/lockheed/data/ms2/documents/procerus/Kestral-Flight-Systems-brochure.pdf

[6] [Online]. Available: http://www.micropilot.com/

[7] T. W. Carnes, "A low cost implementation of autonomous takeoff and landing," Master's thesis, Virginia Commonwealth University, 2014.

[8] J. E. Ortiz, "Development of a low cost autopilot system for unmanned aerial vehicles," Master's thesis, Virginia Commonwealth University, 2010.

[9] Texas Instruments. Pcb design guidelines for 0.5mm package-on-package applications processor, part i. [Online]. Available: http://www.ti.com/lit/an/sprabb3/sprabb3.pdf

[10] [Online]. Available: https://en.wikipedia.org/wiki/Joint_Test_Action_Group

[11] [Online]. Available: http://www.dji.com/product/phantom

[12] P. Project. Paparazzi. [Online]. Available: http://wiki.paparazziuav.org/wiki/Main_Page

[13] (2013, 02) Miniature spi digital barometer. Freescale Semiconductor. [Online]. Available: http://www.freescale.com/files/sensors/doc/data_sheet/MPL115A1.pdf

[14] P. T. Dominik Honegger, Lorenz Meier and M. Pollefeys. An open source and open hardware embedded metric optical flow an open source and open hardware embedded metric optical flow cmos camera for indoor and outdoor applications. [Online]. Available: http://people.inf.ethz.ch/dominiho/publications/ICRA_2013_px4flow.pdf

[15] (2014, Nov). [Online]. Available: http://www.cloudcaptech.com/Sales%20and%20Marketing%20Documents/Piccolo%20Ground%20Station%20Data%20Sheet.pdf

[16] [Online]. Available: http://www.cloudcaptech.com/Sales%20and%20Marketing%20Documents/Piccolo%20II%20Data%20Sheet.pdf

[17] [Online]. Available: http://www.cloudcaptech.com/Sales%20and%20Marketing%20Documents/Piccolo%20SL%20Data%20Sheet.pdf

[18] Cloud Cap Technology Piccolo Nano. [Online]. Available: http://www.cloudcaptech.com/Sales%20and%20Marketing%20Documents/Piccolo%20Nano%20Data%20Sheet.pdf

[19] Kestrel v3.0 / vtol platforms. [Online]. Available: http://www.uadrones.net/systems/research/acrobat/110208.pdf

[20] MicroPilot. Mp2x28 family of autopilots. [Online]. Available: http://www.micropilot.com/pdf/brochures/brochure-MP2x28.pdf

[21] J. C. McBride, "Flight Control System for Small High-Performance UAVs," Master's thesis, Virginia Commonwealth University, May 2010.

[22] R. C. DeMott II, "Development of a flexible fpga-based platform for flight control system research," Master's thesis, Virginia Commonwealth University, 2010.

[23] G. L. Ward, “Design of a small form-factor flight control system,” Master’s thesis, Virginia Commonwealth University, 2014.

[24] [Online]. Available: http://www.chibios.org/dokuwiki/doku.php

[25] M. T. Leccadito, “A Kalman Filter Based Attitude Heading Reference System Using a Low Cost Inertial Measurement Unit,” Master’s thesis, Virginia Commonwealth University, August 2013.

[26] ST. (2013, Jun) STM32F405xx/STM32F407xx Datasheet (DM00037051). [Online]. Available: http://www.st.com/st-web-ui/static/active/en/resource/technical/document/datasheet/DM00037051.pdf

[27] [Online]. Available: http://www.futaba-rc.com/sbus/

[28] [Online]. Available: https://developer.mbed.org/users/Digixx/notebook/futaba-s-bus-controlled-by-mbed/

[29] Sn74lvc245a octal bus transceiver with 3-state outputs. Texas Instruments. [Online]. Available: http://www.ti.com/lit/ds/symlink/sn74lvc245a.pdf

[30] Tps5450 5-a, wide input range, step-down converter. [Online]. Available: http://www.ti.com/lit/ds/symlink/tps5450.pdf

[31] M2831 high frequency 1.5a load - step-down dc-dc regulator lm2831 high frequency 1.5a load - step-down dc-dc regulator. [Online]. Available: http://www.ti.com/lit/ds/symlink/lm2831.pdf

[32] Mic5219: 500ma-peak output ldo regulator. [Online]. Available: http://www.micrel.com/_PDF/mic5219.pdf

[33] (2009, July) An 583: Designing power isolation filters with ferrite beads for altera fpgas. [Online]. Available: https://www.altera.com/content/dam/altera-www/global/en_US/pdfs/literature/an/an583.pdf

[34] L78 positive voltage regulator ics. [Online]. Available: http://www.mouser.com/ds/2/389/CD00000444-249828.pdf

[35] Very low quiescent current bicmos voltage regulator. [Online]. Available: http://www.st.com/web/en/resource/technical/document/datasheet/CD00186925.pdf

[36] (2015, June) Tps6211x 17-v, 1.5-a, synchronous step-down converter tps6211x 17-v, 1.5-a, synchronous step-down converter tps6211x 17-v, 1.5-a, synchronous step-down converter tps6211x 17-v, 1.5-a, synchronous step-down converter. [Online]. Available: http://www.ti.com/lit/ds/symlink/tps62112.pdf

[37] M.-E. Division. (2013, September) Micro battery product catalogue 2013-2014. [Online]. Available: http://www.sii.co.jp/compo/catalog/battery_en.pdf

[38] GPS and GNSS Module Overview Guide. [Online]. Available: http://media.digikey.com/pdf/Data%20Sheets/Linx%20Technologies%20PDFs/GPS&GNSS_ModuleOverview_Guide_2-19-15.pdf

[39] (2010, August) Low-power, high-efficiency, single/dual, rail-to-rail i/o op amps. [Online]. Available: http://datasheets.maximintegrated.com/en/ds/MAX9613-MAX9615.pdf

[40] (2010, June) Integrated silicon pressure sensor, on-chip signal conditioned, temperature compensated and calibrated. [Online]. Available: http://cache.freescale.com/files/sensors/doc/data_sheet/MP3V5004G.pdf

[41] (2015, July) Mp3h6115a, 15 to 115 kpa, absolute, integrated pressure sensor. [Online]. Available: http://www.freescale.com/files/sensors/doc/data_sheet/MP3H6115A.pdf

[42] (2013, October). [Online]. Available: http://www.meas-spec.com/downloads/MS4525DO.pdf

[43] Microchip. (2010) 25LC512 Datasheet (DS22065C). [Online]. Available: http://ww1.microchip.com/downloads/en/DeviceDoc/22065C.pdf

[44] T. Instruments. Dp83848x phyter mini / ls single port 10/100 mb/s ethernet transceiver. [Online]. Available: http://www.ti.com/lit/ds/symlink/dp83848j.pdf

[45] P. Electronics. Pulsejack 1x1 tab-down rj45.

[46] Future Technology Devices International Ltd. (2010) FT2232D Dual USB to Serial UART/FIFO IC. [Online]. Available: http://www.ftdichip.com/Support/Documents/DataSheets/ICs/DS_FT2232D.pdf

[47] InvenSense. (2013, September) Mpu-9150 product specification revision 4.3. [Online]. Available: http://www.inertialelements.com/docs/PS-MPU-9150A-00v4_3.pdf

[48] Fgpmmopa6h gps standalone module data sheet. [Online]. Available: https://www.adafruit.com/datasheets/GlobalTop-FGPMMOPA6H-Datasheet-V0A.pdf

[49] (2015) XBee PRO 900. [Online]. Available: http://www.digi.com/products/wireless-wired-embedded-solutions/rf-modules/xbee-rf-modules/xbee-proprietary-rf-modules/xbee-pro-900hp#specs

[50] (2015, January) Sn74lvc244a octal buffer/driver with 3-state outputs. [Online]. Available: http://www.ti.com/lit/ds/symlink/sn74lvc244a.pdf

[51] "High-speed pcb design considerations," Lattice Semiconductor Corporation, Tech. Rep., April 2011.

[52] L. S. Corporation. (2004, May) Power decoupling and bypass filtering for programmable devices. [Online]. Available: http://www.latticesemi.com/~/media/LatticeSemi/Documents/ApplicationNotes/PT/PowerDecouplingandBypassFilteringforProgrammableDevices.PDF

[53] [Online]. Available: http://www.blacksphere.co.nz/main/blackmagic

[54] [Online]. Available: https://www.raspberrypi.org/products/raspberry-pi-2-model-b/